



Universiteit
Leiden
The Netherlands

Systematic identification of silencers in human cells

Pang, B.X.; Snyder, M.P.

Citation

Pang, B. X., & Snyder, M. P. (2020). Systematic identification of silencers in human cells. *Nature Genetics*, 52(3), 254-263. doi:10.1038/s41588-020-0578-5

Version: Publisher's Version

License: [Creative Commons CC BY 4.0 license](#)

Downloaded from: <https://hdl.handle.net/1887/3627049>

Note: To cite this publication please use the final published version (if applicable).



Systematic identification of silencers in human cells

Baoxu Pang^{1,2} and Michael P. Snyder¹✉

The majority of the human genome does not encode proteins. Many of these noncoding regions contain important regulatory sequences that control gene expression. To date, most studies have focused on activators such as enhancers, but regions that repress gene expression—silencers—have not been systematically studied. We have developed a system that identifies silencer regions in a genome-wide fashion on the basis of silencer-mediated transcriptional repression of caspase 9. We found that silencers are widely distributed and may function in a tissue-specific fashion. These silencers harbor unique epigenetic signatures and are associated with specific transcription factors. Silencers also act at multiple genes, and at the level of chromosomal domains and long-range interactions. Deletion of silencer regions linked to the drug transporter genes *ABCC2* and *ABCG2* caused chemo-resistance. Overall, our study demonstrates that tissue-specific silencing is widespread throughout the human genome and probably contributes substantially to the regulation of gene expression and human biology.

Less than 2% of the 3 billion base pairs in the human genome codes for proteins^{1,2}. The majority is non-protein-coding and includes repeat regions, noncoding RNAs, gene introns and other intergenic regions¹. Individual laboratories, as well as large consortia such as Encyclopedia of DNA Elements (ENCODE) and Roadmap Epigenomics, have made enormous contributions to annotating the noncoding genome with epigenetic modifications and transcription factor binding sites^{3–8}. Based on the profiling of epigenetic modifications, the human genome can be categorized into distinct functional units such as enhancers, insulators and promoters^{9,10}. Disruption of noncoding regulatory regions has been shown to have deleterious effects and cause cancer^{11–14}. However, most research has focused on defining enhancers, insulators and promoters^{15–19}. Although silencers are an important class of regulatory elements²⁰, to date most studies have been performed on identification and characterization of individual silencer regions (for example, those that regulate *CD4* gene transcription during T-cell development^{21–25}), and high-throughput methods have not been described to systematically identify genomic silencers. As such, we do not know how many silencers exist, how they operate at the level of chromosomal domains or whether they exhibit ubiquitous or cell-type-specific activity.

Here we present a method to identify and define the function of silencer regions in a systematic and high-throughput fashion. This method measures the repressive ability of silencer elements (ReSE) by screening for genomic fragments that repress the transcription of an inducible cell death protein. Using this method, we identified more than 5,000 tissue-specific candidate silencer elements in the human genome. These silencers are preferentially located in repressed and/or weakly transcribed regions and share unique epigenetic marks. They operate in topologically associating domains (TADs) and participate in long-range interactions. Deletion of silencers linked to drug transporter genes led to transcriptional up-regulation of these genes and promoted chemotherapy resistance, suggesting that genetic variation in silencer regions may impact both biology and personalized medicine.

Results

Identification of silencers using ReSE. To systematically discover silencer regions in the human genome, a high-throughput ReSE lentiviral screen system was developed (Fig. 1a). In this system, genomic regions are cloned upstream of the EF-1 α promoter that drives the expression of a modified caspase 9 fused to an FK506 binding protein (FKBP-Casp9)^{26,27}. Following the addition of dimerizer molecule AP20187, the expressed caspase 9 is activated to induce apoptosis^{26,27}. The system was designed such that if silencers are inserted, they will repress the transcription of the FKBP-Casp9 gene in the cells, and these cells will not undergo apoptosis. Surviving cells are then expanded, and candidate inserts sequenced and mapped to the genome. This method allows for the systematic identification of silencer regions.

Currently, because it is difficult to screen the entire human genome with small genomic fragments in a lentiviral assay, an enrichment strategy was used. It has been shown that 94.4% of the combined transcription factor chromatin immunoprecipitation sequencing (ChIP-seq) peaks from the ENCODE project fall within accessible regions²⁸. Because many of these transcription factors are associated with transcriptionally repressive activities, we expected that at least some silencers might lie in accessible chromatin regions, as shown for the regulation of the gene *CD4* (refs. 21–25). These silencers would probably harbor regulatory proteins rather than simply be regions that are globally repressed through general heterochromatin mechanisms.

Accessible chromatin regions enriched by formaldehyde-assisted isolation of regulatory elements (FAIRE)²⁹ from chronic myeloid leukemia K562 cells were isolated to construct the ReSE screen library (Supplementary Fig. 1). Briefly, accessible chromatin regions of 200 base pairs (bp) prepared from K562 cells were cloned into the ReSE lentiviral plasmids and a library of <177,000 independent regions (covering 1% of the human genome; distribution in Supplementary Fig. 2) was constructed and used as the screening library. The library was transduced into K562 cells in two independent replicate experiments, and AP20187 was added to induce

¹Department of Genetics, Stanford University, Stanford, CA, USA. ²Department of Cell and Chemical Biology, Leiden University Medical Center, Leiden, the Netherlands. ✉e-mail: mpsnyder@stanford.edu

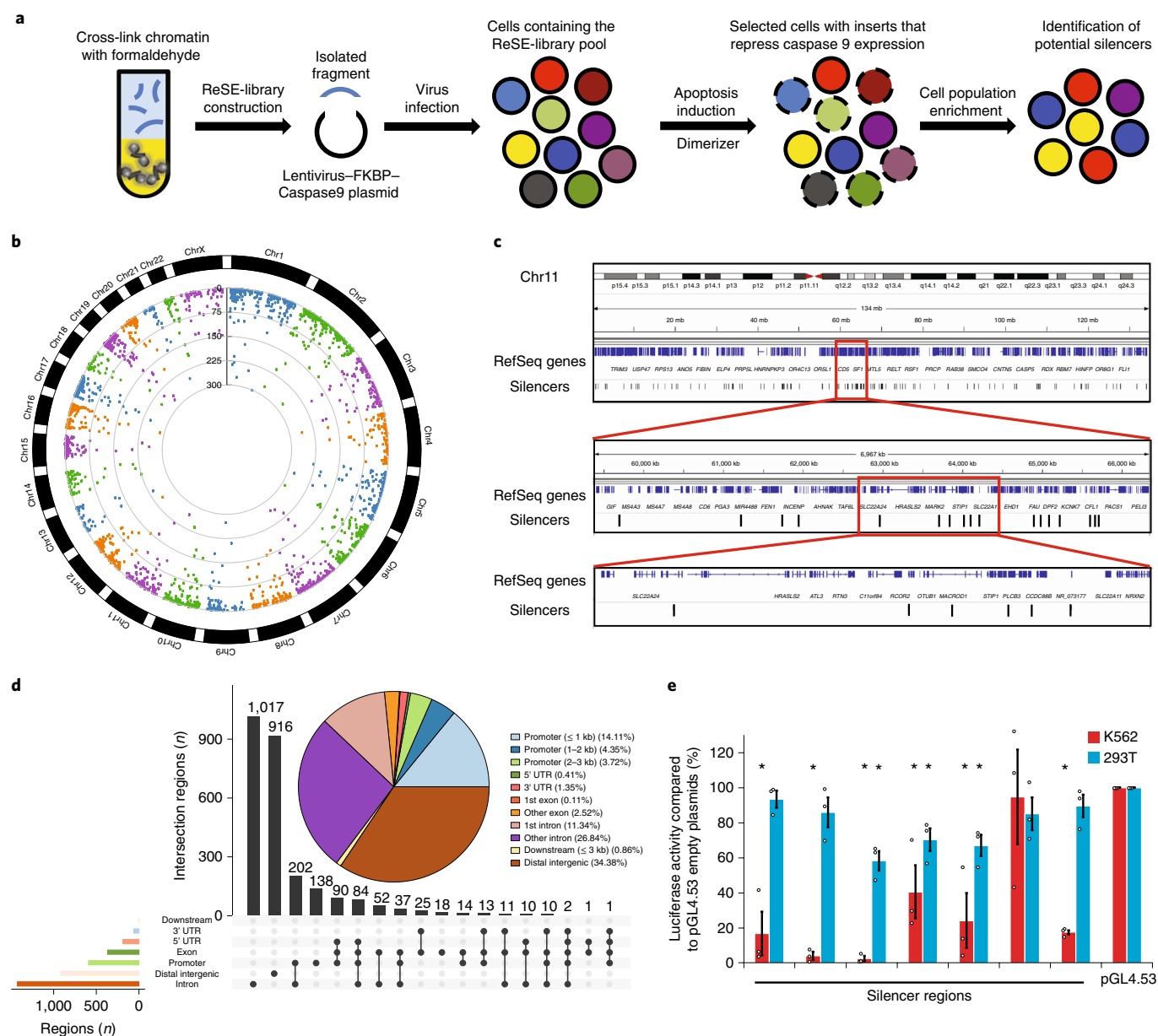


Fig. 1 | Identification of silencers using the ReSE screen. a, Outline of the screen design. Candidate sequences are cloned in front of the EF-1 α promoter that drives the expression of a modified caspase 9 fused to FKBP-Casp9. Following the addition of a dimerizer molecule, the expressed caspase 9 is activated to induce apoptosis unless a potential silencer fragment is inserted. Enriched fragments representing potential silencers are identified when compared to sequences from cells not treated with the dimerizer. **b**, ReSE screen results from two biological replicate experiments in K562 cells. Each dot represents one tested fragment. The position of each dot indicates the location of each fragment within the respective chromosome. The height of the dot indicates the $-\log_{10}(\text{FDR})$ of enrichment of the ReSE fragments after the induction of apoptosis compared with cells not treated with dimerizer. The cutoff value of FDR is 0.01. See Methods for detailed information. **c**, Snapshot of distribution of silencers in K562 cells. Chromosome 11 (Chr11) is used as an example. **d**, Distribution of significantly enriched silencer regions from K562 cells in the genome. The pie chart indicates the distribution of silencers in genomic features; the bar plot indicates the distribution of silencers in overlapping annotation features in the genome. **e**, Luciferase assays to determine the repressive activity of silencers identified from K562 cells. Silencer regions were cloned by PCR from the genomic DNA of K562 cells, then inserted upstream of the promoter of the luciferase reporter plasmid pGL4.53. 293T cells were used as the cell line to control for cell-type-dependent repressive activity, and empty pGL4.53 plasmid was used as the control for baseline luciferase activity. The y axis represents the percentage of luciferase activity compared to pGL4.53 empty plasmids in the respective cells ($n=3$ biological independent samples; bars show mean value \pm s.e.m.; * $P < 0.05$, calculated using two-sided Student's t -test). All precise P values are provided in the Source Data.

apoptosis (Supplementary Fig. 3, further details in Methods). The surviving cells were grown and the inserts were sequenced before and after selection. Because the screen has considerable background cell survival during the initial puromycin selection and subsequent apoptosis induction, fold enrichments are variable due to both this

and the low read counts (see Methods). Nonetheless, the results from the replicate experiments correlated (Extended Data Fig. 1a) although only a small percentage of the potential fragments was consistently enriched between replicates when fold change was considered (Supplementary Fig. 4).

To reliably identify significantly enriched silencers, an algorithm based on a negative binomial model was adapted³⁰, as used previously in CRISPR screening and other RNA-sequencing (RNA-seq) differential analyses^{30–32}. This led to the identification of 2,664 potential silencer regions with a false discovery rate (FDR) cutoff of 0.01 in K562 cells (Fig. 1b,c, Extended Data Fig. 1b, Supplementary Fig. 5 and Supplementary Table 1). The majority of these potential silencer regions were in promoter regions, introns and intergenic regions (Fig. 1d). To validate the transcriptional repressive activity of the identified silencer regions, seven regions identified from the screen with the lowest FDR were cloned upstream of a luciferase plasmid with a phosphoglycerate kinase (PGK) promoter. Very strong repressive activity was observed from the silencer fragments in K562 cells in six out of seven cases (Fig. 1e). In addition, testing of five silencers from the bottom of our silencer list revealed that three showed significant repressive activity (Extended Data Fig. 2a), suggesting that the high threshold used for calling positives (FDR=0.01) was adequate. The majority of randomly selected regions (eight out of nine) from the library did not show repressive ability (Extended Data Fig. 2b). These data indicate that most fragments identified in our screen are silencers and, in addition, suggest that the activity of most silencers was not limited to the specific promoter used in the initial screen (that is, the EF-1 α promoter in Fig. 1a).

To test whether the silencers can repress their native endogenous genes, three silencer regions from Fig. 1e were deleted from their native loci. Silencer regions located in the intron regions of genes *HRH1*, *SYNE2* and *CDH23* were deleted using paired CRISPR guide RNAs that targeted both sides of the individual silencer region. K562 silencer knockout clones were isolated, and significant up-regulation of the respective genes was observed in each case (Extended Data Fig. 3). These data indicate that silencers identified in the ReSE screen repress the transcription of their nearby endogenous genes.

ReSE identifies tissue-specific and conserved silencers. Since large-scale analysis of silencers has not previously been performed, we wanted to determine whether they were common across cell types or whether they function in a tissue-specific manner, similarly to enhancers^{33,34}. We used the same screening library to test whether a different pool of silencers was enriched during differentiation of K562 cells; the rationale was that, if most silencers are common across cell types, we would isolate many of the same DNA sequences found in the K562 screen. If the silencers are cell-type specific, the overlap should be modest. K562 cells were treated with phorbol 12-myristate 13-acetate (PMA) to induce megakaryocytic differentiation. Repeating the ReSE screen in these PMA-treated cells identified a different set of 1,245 silencers compared to those identified in the original K562 cells (Extended Data Fig. 4 and Supplementary Table 2). This result suggests that silencers may function in a tissue-specific manner.

To further test this observation, we repeated the ReSE screen on HepG2 cells (of hepatocyte origin) using the same ReSE library made from the K562 FAIRE enrichment. Again the rationale was that if the two cell types shared common silencers there would be substantial overlap in the silencers between both cell types. Two independent biological ReSE screens of HepG2 cells led to the identification of 1,662 potential silencer regions with FDR=0.01 (Fig. 2a, Extended Data Figs. 5 and 6, Supplementary Fig. 6 and Supplementary Table 3). Although these silencer regions shared a similar overall genomic distribution with K562 cells (Extended Data Fig. 6b), only a small fraction (>2% of the total) of the silencer regions was shared between these two cell lines, indicating that the majority of the silencers that we identified, similarly to enhancers, may exert their function in a tissue-specific fashion (Fig. 2b and Supplementary Fig. 6b). However, as we applied a very stringent FDR cutoff to identify silencers in the respective cell lines, we may

have underestimated the percentage of conserved silencers among different tissues. Nonetheless, the data suggest that many silencers may be tissue specific.

We next directly investigated whether the small percentage of the shared silencers found in K562 and HepG2 cells might be ubiquitous silencers and act in different cell types. To examine this possibility, seven of the silencer regions shared by both K562 and HepG2 screens were tested using the luciferase assay, of which three were found to be repressive in both cell types (Fig. 2c). In addition, repression activity was also observed for five out of the seven common regions tested in 293T cells, suggesting these regions may be cell-type-independent silencers. It should be noted that silencers were called using a stringent algorithm within individual cell lines, and the false-negative rate may be higher when comparing silencers among cell lines; certain top-ranked silencers from HepG2 cells also showed some repressive activity in K562 cells (Extended Data Fig. 6a). We also noted that the FDR was higher in HepG2 cells, presumably because the screen library was made from FAIRE regions of K562 cells and we might not have identified the strongest silencers in HepG2 cells. Overall, our current data suggest that the majority of silencers may be cell-type specific, with a small number operating in two or more cell lines (Fig. 1e and Extended Data Figs. 2a and 6a).

Since the majority of silencers identified by ReSE screen may function in a tissue-specific manner, we further tested whether silencers associate with genes in unique pathways. Pathway analyses using ingenuity pathway analysis revealed unique pathways with strong confidence (that is, lower *P* value) for the proximal genes associated with silencers identified from the different cell types. We employed two different methods to identify proximal genes that may be regulated by silencers in K562 and HepG2 cells: (1) the presence of silencers only in the promoter regions (10 kb surrounding transcription starting sites (TSS); Supplementary Tables 4 and 5); and (2) the presence of silencers in both promoter regions (1 kb surrounding TSS, which is a more stringent definition)^{35,36} and gene bodies, since many silencers were enriched in the intron regions (Fig. 2d,e and Supplementary Tables 6 and 7). When the presence of silencers in both promoters and gene bodies was considered, in K562 cells, protein kinase A signaling and actin cytoskeleton signaling pathways were among the top pathways enriched for silencer-associated genes (Fig. 2d and Supplementary Table 6). Since K562 cells are a myeloid cell line growing in suspension culture, it is likely that the actin cytoskeleton signaling pathway is repressed or poised for activation as compared to adherent cells³⁷. In contrast, neuronal pathways and cardiac pathways were the top genes that lay near silencers isolated from HepG2 cells (Fig. 2e and Supplementary Table 7). Such pathways are also expected to be repressed, since HepG2 cells were derived from a hepatic cell lineage.

Silencers consist of unique genetic and epigenetic signatures.

Functional regulatory elements are usually present in defined chromatin states^{10,38}. For instance, enhancer regions are often marked by modifications such as H3K4me1 and H3K27ac¹⁰. To determine the chromatin states of silencer regions identified by ReSE, the recovered regions from K562 and HepG2 were first classified based on the ENCODE chromatin definitions^{10,39}. More than one-quarter of the silencers were enriched in either the weak transcription chromatin state ($P < 2.2 \times 10^{-16}$, one-sided binomial test using the screen library as the background) or the repressed state ($P = 3.325 \times 10^{-5}$, one-sided binomial test; Fig. 3a and Extended Data Fig. 7a). This indicates that silencers may be associated with specific chromatin modifications that might be necessary for exertion of their silencing function.

To further examine the epigenetic marks and transcription factors that may be enriched in the silencer regions, a permutation-based test was performed to associate silencer regions with available datasets from the ENCODE project^{3,40}. When histone

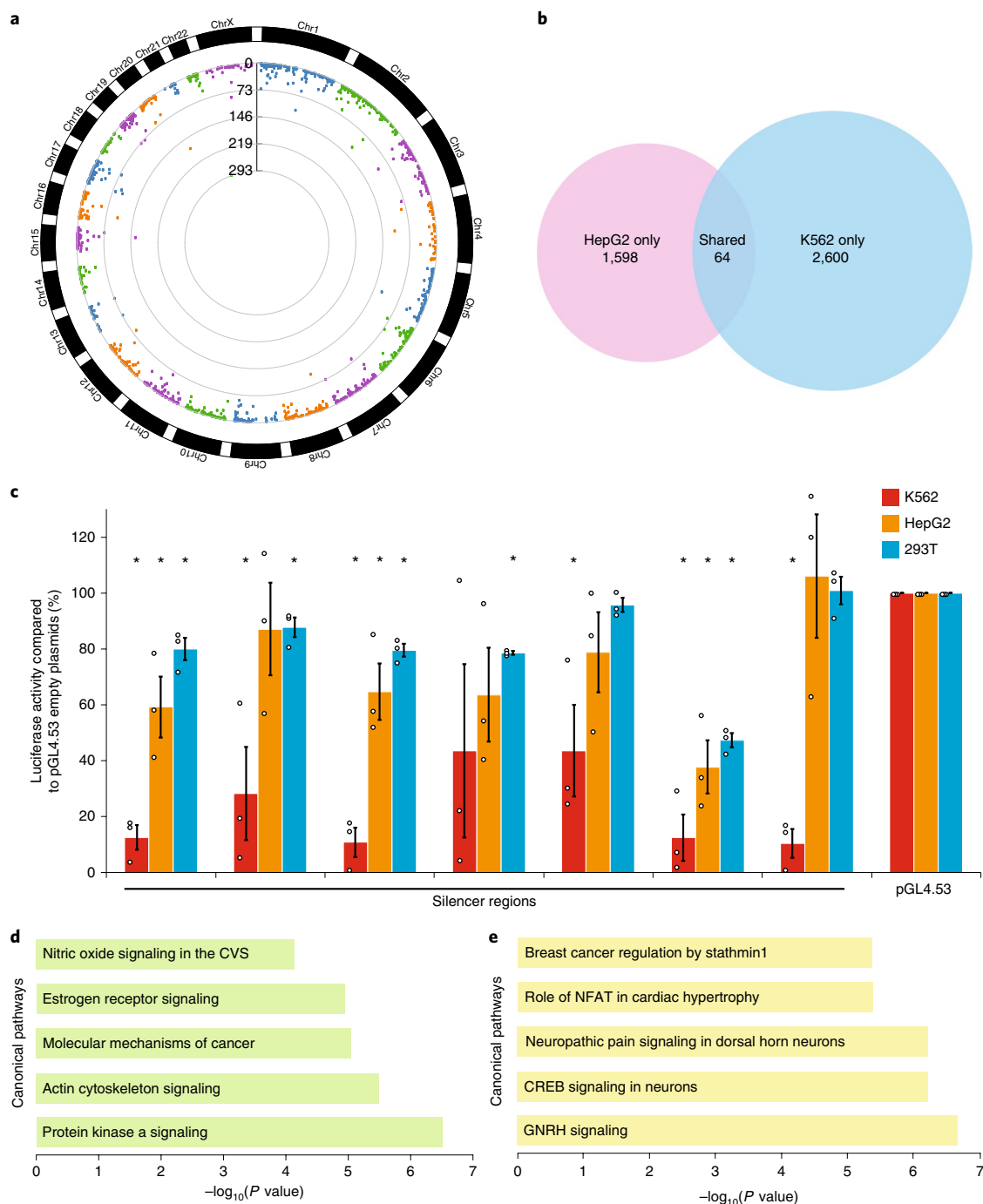


Fig. 2 | Conserved and tissue-specific distribution of silencers. **a**, ReSE screen results from two biological replicate experiments in HepG2 cells. Each dot represents one tested fragment, its position indicating the location of that fragment within the respective chromosome. Dot height indicates $-\log_{10}(\text{FDR})$ of enrichment of ReSE fragments after induction of apoptosis compared with cells not treated with dimerizer. Cutoff value of $\text{FDR} = 0.01$. See Methods for detailed information. **b**, Comparison of silencer regions identified from K562 and HepG2 cells. Overlapping was not random, as determined by permutation tests (n of testing = 20,000, adjusted $P = 0.00005$). **c**, Luciferase assays to determine the repressive activity of shared silencers from K562 and HepG2 cells. Silencer regions were cloned by PCR from the genomic DNA of K562 cells into luciferase reporter plasmid pGL4.53. 293T cells were used as the control cell line and empty pGL4.53 plasmid was used as the control for baseline luciferase activity. The y axis represents the percentage of luciferase activity compared to that with pGL4.53 empty plasmids in the respective cells ($n = 3$ biological independent samples; bars show mean value \pm s.e.m.; * $P < 0.05$, calculated using two-sided Student's t -test). **d, e**, Top canonical pathways enriched in gene sets containing silencers in K562 cells (**d**) and in HepG2 cells (**e**). CVS, cardiovascular system; NFAT, nuclear factor of activated T cells; CREB, cAMP response element-binding protein; GNRH, gonadotropin-releasing hormone. All precise P values are provided in the Source Data.

marks were analyzed, H4K20me-modified chromatin was significantly co-associated with silencers from both K562 and HepG2 cells (Fig. 3b and Extended Data Fig. 7b). The role of H4K20me

modification remains complex, as both transcriptional repression and activation have been associated with this mark⁴¹. Interestingly, different heterochromatin histone marks, each associated with gene

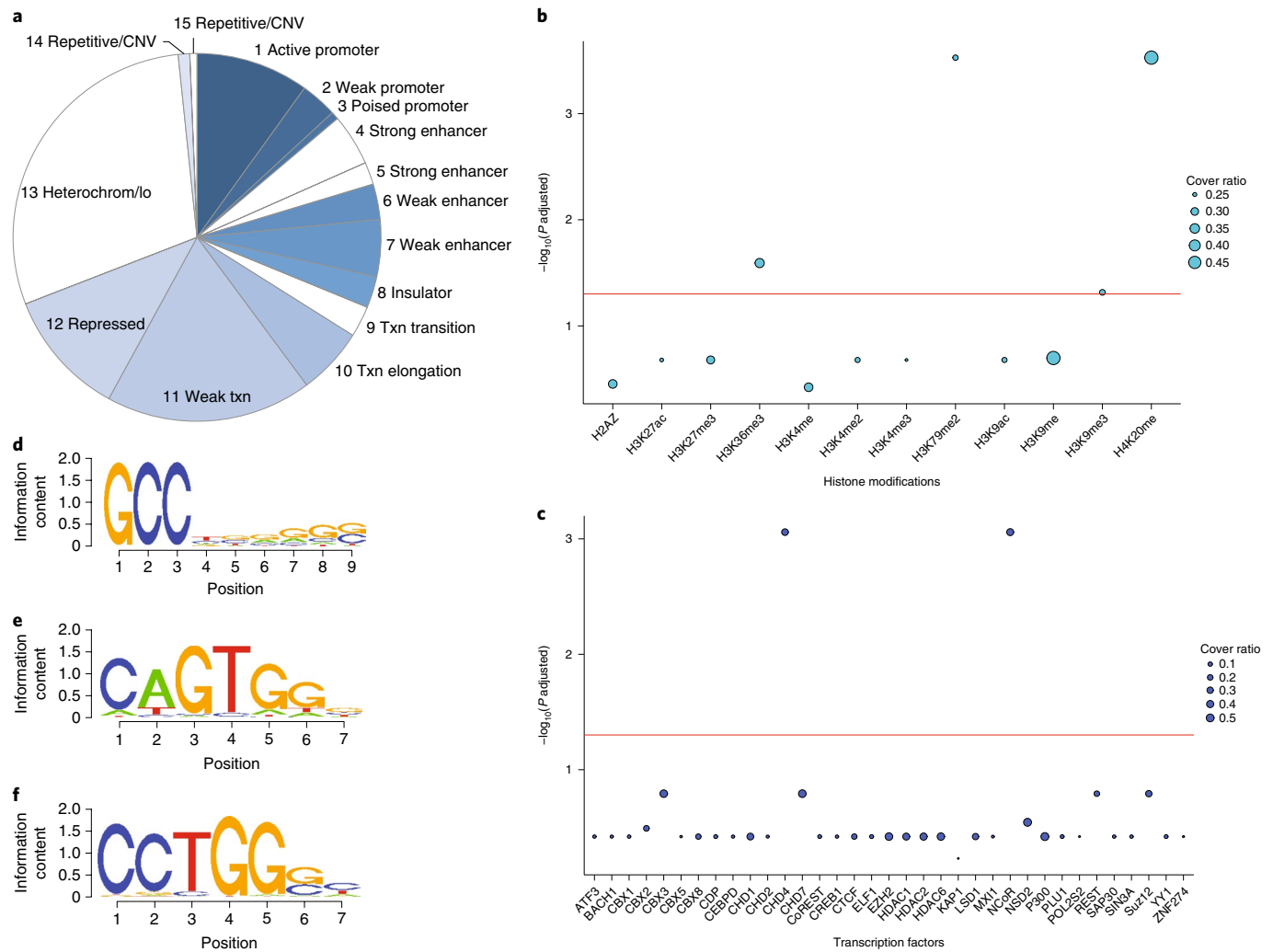


Fig. 3 | Unique signatures in silencer regions. **a**, Distribution of silencer regions in respective chromatin states in K562 cells. Txn, transcription; Repressed, Polycomb repressed; lo, low signal; CNV, copy number variation. Colored wedges indicate chromatin states significantly enriched compared to library background distribution ($P < 0.001$, one-sided binomial test). **b, c**, Association of histone modifications (**b**) and transcription factors (**c**) with silencers in K562 cells. The y-axis indicates the significance of the enrichment of histone modifications with silencer fragments. Circle size indicates the ratio of silencers covered by the respective histone modification (scale, 0–1). **b, c**, Enrichment analysis is based on permutation tests using 20,000 random permutations. P values were calculated and multiple comparison corrections were computed using the Benjamini–Hochberg procedure. The red line shows the cutoff of adjusted $P < 0.05$. **d–f**, Examples of top known motifs (K562 AP2 (**d**), K562 KLF12 (**e**) and K562 de novo (**f**)) present in silencer regions in K562 cells. All precise P values are provided in the Source Data.

inactivation, were found to associate with silencers isolated from K562 (H3K9me3; Fig. 3b) and HepG2 cells (H3K27me3; Extended Data Fig. 7b). This difference may be due to the fact that the initial silencer screen library was constructed from K562 cells, and these silencers may represent a different pool in HepG2 cells. In addition to histone marks related to silencing, H3K36me3 and H3K79me2, both active histone marks, were also significantly associated with silencers. It has been suggested that, when combined with other histone marks, active marks such as H3K36me3 can be found in heterochromatin regions⁴². This finding is also consistent with the observation that the identified silencers are enriched in weak transcription chromatin states (Fig. 3a and Extended Data Fig. 7a). We note that the selected silencer regions that were targeted for knock-out in K562 cells (Extended Data Fig. 3) all showed the presence of the H4K20me modification (Supplementary Fig. 7), further indicating that in these representative silencer regions, this mark may be associated with gene silencing (Fig. 3b). In addition, these silencers also showed overlap with H3K27me3 or H3K9me3 (Supplementary

Fig. 7), indicating either a weak transcription chromatin state or a repressed state (Fig. 3a).

Regulatory proteins that participate in repression might be enriched in silencers. Therefore, a permutation-based co-association test was performed between silencers and regions bound by transcription factors in both K562 and HepG2 cells^{3,40}. In K562 cells, CHD4 and NCoR were significantly enriched in silencer regions (adjusted $P = 0.0008$; Fig. 3c). A different set of transcription factors, for example EZH2 and REST, were enriched in HepG2 cells (Extended Data Fig. 7c). This probably reflects the cell-type specificity of silencers, because different cell types presumably use different proteins to regulate silencers. While it is likely that different cell types may employ different proteins for silencing, it is also possible that other, unidentified, silencer proteins are common to different cell types. It is worth noting that, among the transcription factors tested, KAP1 and ZNF274 were not associated with silencers identified using our open chromatin screen. This is likely because they are primarily associated with inaccessible chromatin²⁸, which

is less likely to be enriched in the screen library. As controls, p300, which is usually associated with transcription activation³³, or Pol2S2 (phosphorylation of serine 2 on CTD of RNA polymerase II), which is usually associated with active transcription⁴³, were also not enriched with silencers.

To identify other potential novel factors that may recognize the silencer regions identified by our ReSE screen, motif analyses were performed using SeqPos⁴⁴. The top known motif identified in both K562 and HepG2 cells was the AP2 binding domain (Fig. 3d and Extended Data Fig. 8), with $P=10^{-358}$ and $P=10^{-225}$, respectively). Although the role of AP2 family members in transcription repression has previously been shown^{45,46}, a general repressive activity of AP2 in different tissues has not been established. Furthermore, the motif of another known transcription repressor, KLF12, was also enriched in K562 cells (Fig. 3e)⁴⁷. In addition to motifs with known binding factors, many de novo motifs were also identified in both K562 (Fig. 3f) and HepG2 cells (Extended Data Fig. 8b). These motifs are GC-rich, similarly to AP2 motifs. Our data indicate that there may be unique factors that function in silencer regions that are yet to be identified.

Silencers regulate proximal endogenous genes to promote chemo-resistance. We next examined whether the silencer regions identified by the ReSE screen have direct biological effects. Pathway analyses based on genes that harbor silencers, in both the promoter and gene body regions (Fig. 2d and Supplementary Table 6), revealed that silencers were enriched in genes for an ABC drug transporter pathway in K562 cells (Supplementary Fig. 8; $-\log(P)=2.671$). Within the intron regions of the drug transporter genes *ABCC2* (on chromosome 10) and *ABCG2* (on chromosome 4) there exist two potential silencers (Supplementary Fig. 9). It is possible that these silencers affect the transcription of those genes and thus participate in response to drug treatment (Fig. 4a). Luciferase assays showed that these silencer regions have repressive activity, and they repressed the transcription of the pGL4.53 reporter by 50% (*ABCC2* locus silencer) and 80% (*ABCG2* locus silencer) (Fig. 4b).

The silencers in the *ABCC2* and *ABCG2* loci were targeted with flanking CRISPR gRNAs to delete the regions from the genome (Fig. 4a), and K562 cell clones with the complete knockout of the silencer within *ABCC2* (Fig. 4c) and *ABCG2* (Fig. 4d) were derived. Transcription of genes *ABCC2* and *ABCG2* was significantly up-regulated in these clones, and such up-regulation was unrelated to puromycin selection since control knockout clones did not show this strong increase (Fig. 4e,f; additional clones and comparisons among all individual clones with control knockout clones are shown in Extended Data Fig. 9). In contrast, knocking out the same silencer regions did not induce significant up-regulation of *ABCC2* in 293T cells, or only modestly up-regulated the *ABCG2* gene in 293T cells (Extended Data Fig. 9), in accordance with the luciferase assay in Fig. 4b, further indicating that silencers function in a tissue-specific manner. As a result of the transcriptional up-regulation of drug transporters, these knockout clones are more resistant to chemotherapeutic drug treatments compared to the parental cell line (Fig. 4g), suggesting that silencer regions may affect drug sensitivity.

When local epigenetic modifications were examined, the silencer region in the *ABCC2* gene was marked with H2A.Z and H3K27ac (Supplementary Fig. 9), whereas the silencer region in *ABCG2* overlapped with H3K27me3 and had the H4K20me modification residing nearby (Supplementary Fig. 9). The latter mark is consistent with the results presented in Fig. 3b and Supplementary Fig. 7. In addition, the gene bodies of both *ABCC2* and *ABCG2* were largely covered by H3K27me3 modification, indicating a repressed state of these genes. These two silencer regions were not covered by the H4K20me mark (although the silencer in the *ABCG2* locus showed H4K20me in close proximity).

Silencers regulate transcription in the three-dimensional genome. *Cis*-regulatory elements often regulate not only a single gene but a group of genes within a TAD^{48,49}. To test whether this occurs for the ReSE-identified silencers, Hi-C data from K562 cells were integrated to define the different domains surrounding the silencer within the *ABCC2* gene^{50,51} (Fig. 5a). Hi-C data indicate that one TAD contains the silencer within the *ABCC2* gene in K562 cells (Fig. 5a). Furthermore, in this TAD a chromatin loop connects both the *ABCC2* and *CPN1* genes (Fig. 5b), as defined by chromatin interaction analysis by paired-end tag sequencing (ChIA-PET) assays targeting RAD21 and CTCF⁵². This result raises the possibility that the silencer within the *ABCC2* gene may also regulate the *CPN1* gene.

Transcriptional changes of genes from two topologically distinct domains were thus tested between control and knockout cell lines using quantitative PCR (qPCR) assays. We found that, similarly to enhancers⁴⁹, silencers also acted on genes within the same chromatin loop domain because the *CPN1* gene was significantly up-regulated in the K562 *ABCC2* silencer knockout cell line (12-fold; Fig. 5c, right with yellow bar), in which the *ABCC2* gene was also strongly up-regulated (300-fold; Figs. 4d and 5c). Strong gene up-regulation was confined to only these two genes within the TAD (Fig. 5a, yellow domain containing *ABCC2* gene), in contrast to genes located in a nearby distinct TAD (Fig. 5c, left with blue bar).

To globally identify distal genes that may be regulated by the silencers, capture Hi-C data that profiled interactions with 31,253 promoter regions from human primary blood cells⁵³ were integrated with silencers identified from K562 cells. Since K562 cells resemble a common myeloid progenitor origin that is similar to that of many of the cell types in blood and can be differentiated into many of these cell types, whole-blood data should contain many of these regulatory regions. Silencer regions identified by ReSE in K562 cells interacted with approximately 4,000 promoter regions (Supplementary Table 8; permutation test adjusted $P=4.99 \times 10^{-5}$, $n=20,000$), suggesting that ReSE silencers can directly interact with many promoter regions.

For direct testing of the effect of promoter-silencer interactions in K562 cells, chromosome conformation capture carbon copy (5C) data from ENCODE reporting long-range interactions between promoter regions and distal elements were examined⁵⁴. However, these 5C experiments targeted only 1% of the genome⁵⁴. We intersected 5C data with the silencer regions identified in K562 cells and found five genes that directly interact with silencer regions (Fig. 5d and Extended Data Fig. 10a). Among these interactions, genes *NRXN2*, *TMC4* and *FOXP4* showed extremely low expression (fragments per kilobase exon per million mapped reads (FPKM) < 2) based on RNA-seq data in K562 cells⁵⁵ (Fig. 5d and Extended Data Fig. 10b), and an additional gene, *RASGRP2*, showed low expression (FPKM < 10; Fig. 5d and Extended Data Fig. 10b). When these silencers were removed individually with flanking CRISPR gRNAs in K562 cells, four out of five genes were up-regulated significantly in the respective clones (Fig. 5e). These data further support the suggestion that silencers may also interact with, and regulate, distal genes.

Discussion

Although only approximately 2% of the human genome contains coding sequences that can be translated into proteins, many non-coding regions contain unique sequences that can be recognized by chromatin modifiers and transcription factors as candidate regulatory elements. Although systematic analysis of promoters and enhancers has been performed previously¹⁵⁻¹⁹, a global analysis of silencers has not been described. In our study, a robust screening system, ReSE, was developed to systematically identify silencer elements in the human genome. ReSE utilizes a lentiviral system to test the ability of candidate genomic fragments to repress the

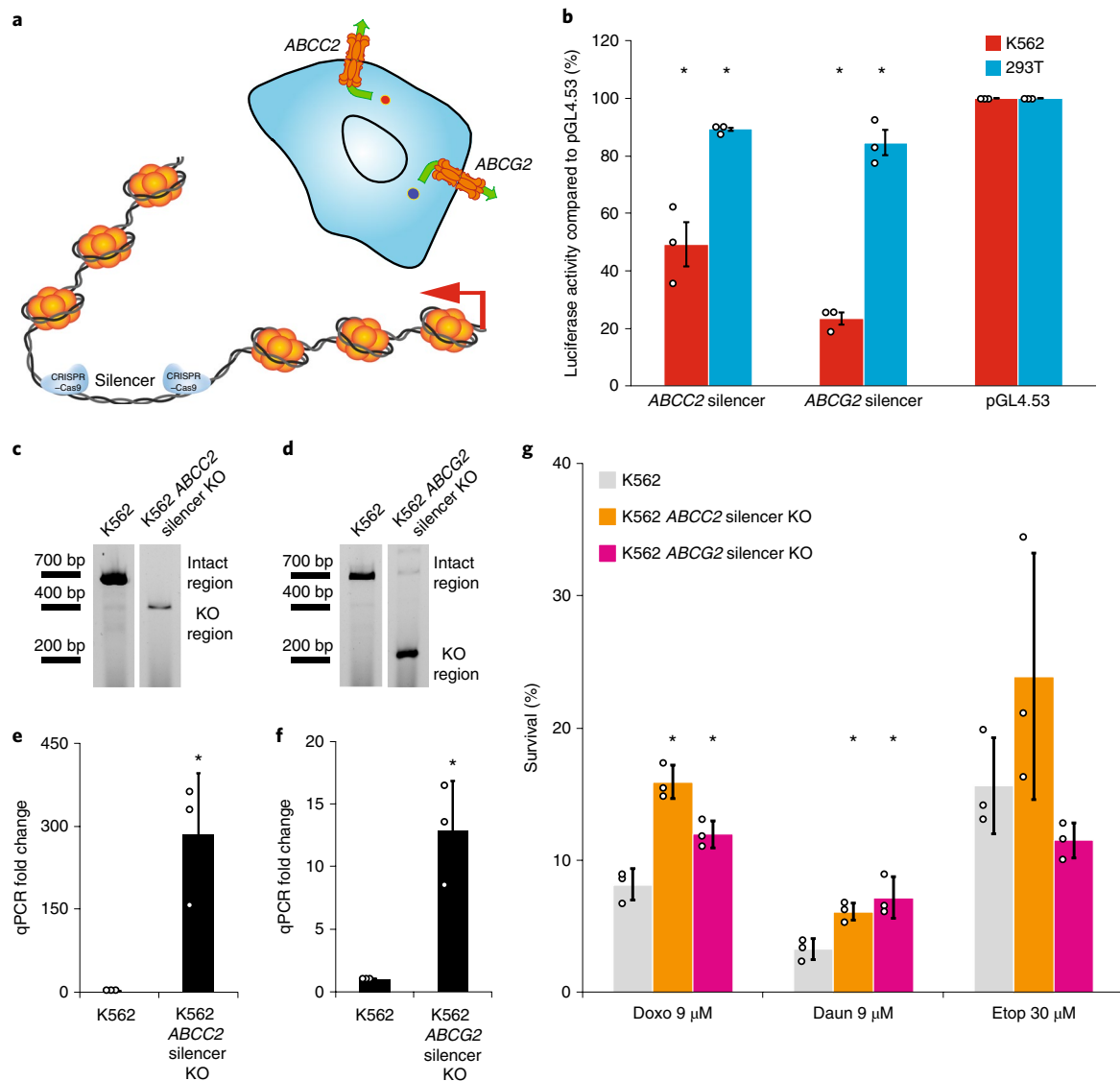


Fig. 4 | Drug resistance regulated by silencer regions. **a**, The genes *ABCC2* and *ABCG2* contain silencers. Upper: the primary known function of *ABCC2* and *ABCG2* in cells, which is to excrete drugs. Lower: the main strategy used by CRISPR-Cas9 to remove silencers from the genome and test their function endogenously. **b**, Luciferase assays to determine the repressive activity of silencers from within genes *ABCC2* and *ABCG2* in K562 cells. 293T cells were used as the control cell line and empty pGL4.53 plasmid was used as the control for baseline luciferase activity. The y axis represents the percentage of luciferase activity compared to that with pGL4.53 empty plasmids in the respective cells ($n=3$ biological independent samples; bars show the mean value \pm s.e.m.; $P < 0.05$, calculated using two-sided Student's *t*-test). **c,d**, Knockout (KO) silencer from genes *ABCC2* (**c**) and *ABCG2* (**d**) using CRISPR-Cas9. PCR result showing the removal of the silencer in two K562 cell clones, which is the representative result of two experiments. The blots were cropped. Full scans of the blots are shown in Source Data. **e,f**, Expression of *ABCC2* (**e**) and *ABCG2* (**f**) quantified by qPCR ($n=3$ biological replicates of the same clones; bars show mean value \pm s.d.; $*P < 0.05$, calculated using two-sided Student's *t*-test). **g**, Drug resistance promoted by the up-regulation of *ABCC2* and *ABCG2* after silencer removal ($n=3$ biological replicates of the same clones; bars show mean value \pm s.d.; $*P < 0.05$, calculated using two-sided Student's *t*-test. Doxo, doxorubicin; Daun: daunorubicin; Etop, etoposide). All precise *P* values are provided in the Source Data.

caspase-based 'kill switch' for the enrichment of potential silencers. In principle, other plasmid-based reporter assays normally used for assessment of enhancers and promoters could also be used to evaluate silencer activity. However, these systems rely on RNA-seq and therefore may be better suited to evaluating activation rather than repression. Despite the fact that fewer genomic regions are individually assayed in the lentiviral system than in other plasmid-based reporter assays, the ReSE lentiviral method can be used to directly select for regions of interest and, in addition, it can overcome the plasmid-transfection-related systematic errors that have been realized recently⁵⁶. Nonetheless, akin to other genome-wide screen systems that are intrinsically noisy, ReSE is also limited by

false-positive and false-negative discovery, and therefore multiple biological replicates are recommended for the screen to increase the statistical power. Although silencer regions may exist in different genomic regions with distinct chromatin structures, to prioritize the testing regions in the human genome, we analyzed open chromatin regions because these are accessible for regulatory factors and might directly exert repressive functions rather than passively be silenced through repressive heterochromatin. The ReSE screen reliably identified silencer fragments in different cell lineages. Our results suggest that many of the silencers that we identified may function in a tissue-specific manner. Nonetheless, it is possible that a large and common pool of shared silencers exists in different tissues, as the

current ReSE screen library was derived from only FAIRE regions of K562 cells and silencers were identified using a stringent cutoff. These data indicate that silencers may play an important role in the development and regulation of tissue differentiation. Unique motifs are present in the silencers that could potentially be recognized by specific factors to exert repressive functions.

Although the majority of silencers may be present in transcriptionally inactive states, presumably some accessible DNA still exists in these chromatin regions that can be isolated using FAIRE^{57,58}. In agreement with this interpretation, silencers were found in the vicinity of genes that are poised for responses or repressed during differentiation. Silencers may possess a unique combination of histone signatures (Fig. 3b, Extended Data Fig. 7b and Supplementary Figs. 7 and 9). Such chromatin states may be the result of the recognition of silencers by repressive transcription factors. Since the current ReSE screen was focused on accessible chromatin regions with a fixed testing size (around 200 bp), the resulting signatures, such as histone modifications, transcription factor associations and sequence motifs, may also be biased towards a particular class of silencers using this library. It is possible that there are many different transcription factors recognizing their respective subclusters of silencers within distinct cell types (Fig. 3c and Extended Data Fig. 7c). Future genome-wide analysis of silencers is required to provide a clearer picture of all possible silencing signatures. Systematic identification of silencers in this way helps to further our understanding of the relationship between repressed chromatin states and gene silencing.

Thus far, investigations of drug responses or disease progression often focus on the coding regions of genes, or known regulatory regions such as promoters and enhancers^{36,59–62}. For instance, a recent CRISPR activation screen targeting promoter regions led to the identification of *ABCG2* as an important drug-resistant player in K562 cells⁶³. We found that deletion of silencers within drug transporter genes *ABCC2* and *ABCG2* also led to the up-regulation of these genes and chemotherapeutic drug resistance, suggesting that silencer-mediated transcription repression may be another layer of regulation contributing to important medical phenotypes. Thus, it is expected that phenotype-associated genetic variants in silencers may affect drug responses (Supplementary Fig. 10), disease initiation and progression, and may be considered as candidates for precision medicine. Furthermore, many diseases are caused by haplo-insufficiency

or insufficient gene expression. This can be effectively rescued by the newly developed CRISPR–dCas9-mediated activation technology, by targeting either the promoter or enhancer regions of the relevant genes^{64–66}. However, unlike the CRISPR–Cas9-mediated genomic editing/correction that requires only transient expression of CRISPR–Cas9 (refs. 36,67), the activation system requires constant expression of CRISPR–dCas9. Therefore such regulation is often reversible^{66,68}, which may not be ideal for future applications in human diseases. As shown in our data, because genomic editing

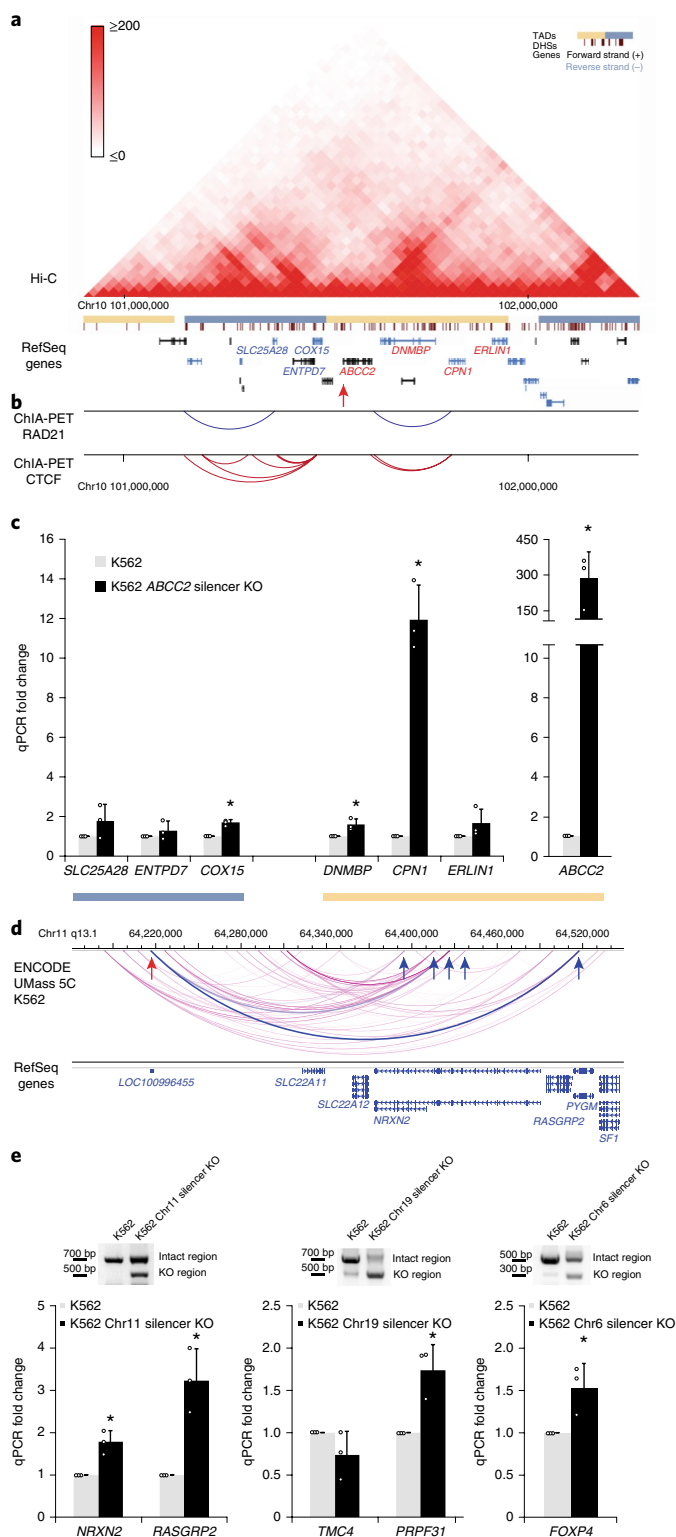


Fig. 5 | Regulation of distal genes by silencers. a, TADs identified by Hi-C data. Arrow indicates the relative location of the silencer. Yellow and blue bars indicate distinct TADs. DHSs, DNase I hypersensitive sites. **b**, ChIA-PET interactions identified using RAD21 (blue, component of cohesin complex) and CTCF (red) surrounding the *ABCC2* gene. **c**, Transcription of genes within different TADs quantified by qPCR. The blue bar indicates genes that do not reside in the same TAD as the *ABCC2* gene; the yellow bar indicates genes that reside in the same TAD as the *ABCC2* gene ($n=3$ biological replicates of the same clones; bars show mean value \pm s.d.; $*P < 0.001$, calculated using two-sided Student's *t*-test). **d**, Direct interaction of silencers with promoters of distal genes from 5C analysis. Red arrow indicates the silencer region, and blue arrow shows the significant interaction region of genes. Significant interaction arcs are highlighted in blue. **e**, Gene up-regulation by removal of promoter-interacting silencers from endogenous regions. Paired CRISPR gRNAs were designed to target both sides of the selected silencers identified in **d** and in Extended Data Fig. 10a. Single clones were selected and verified by PCR (upper), which is the representative result of two experiments. The blots were cropped. Full scans of the blots are shown in Source Data. The expression of respective genes with promoter–silencer interactions was quantified by qPCR (lower) ($n=3$ biological replicates of the same clones; bars show mean value \pm s.d.; $*P < 0.05$, calculated using two-sided Student's *t*-test). All precise *P* values are provided in the Source Data.

of the silencer regions can lead to gene up-regulation, inactivation of silencer regions could be complementary to the CRISPR-dCas9-mediated activation system in the treatment of many diseases. As such, systematic identification of silencers in the genome by using the ReSE screen may not only provide insights into the biology of the genome, but also assist in personalized medicine.

Online content

Any methods, additional references, Nature Research reporting summaries, source data, extended data, supplementary information, acknowledgements, peer review information; details of author contributions and competing interests; and statements of data and code availability are available at <https://doi.org/10.1038/s41588-020-0578-5>.

Received: 15 July 2018; Accepted: 9 January 2020;
Published online: 24 February 2020

References

- Venter, J. C. et al. The sequence of the human genome. *Science* **291**, 1304–1351 (2001).
- Lander, E. S. et al. Initial sequencing and analysis of the human genome. *Nature* **409**, 860–921 (2001).
- Consortium, E. P. An integrated encyclopedia of DNA elements in the human genome. *Nature* **489**, 57–74 (2012).
- Gerstein, M. B. et al. Architecture of the human regulatory network derived from ENCODE data. *Nature* **489**, 91–100 (2012).
- Neph, S. et al. An expansive human regulatory lexicon encoded in transcription factor footprints. *Nature* **489**, 83–90 (2012).
- Djebali, S. et al. Landscape of transcription in human cells. *Nature* **489**, 101–108 (2012).
- Thurman, R. E. et al. The accessible chromatin landscape of the human genome. *Nature* **489**, 75–82 (2012).
- Roadmap Epigenomics, C. et al. Integrative analysis of 111 reference human epigenomes. *Nature* **518**, 317–330 (2015).
- Filion, G. J. et al. Systematic protein location mapping reveals five principal chromatin types in *Drosophila* cells. *Cell* **143**, 212–224 (2010).
- Ernst, J. et al. Mapping and analysis of chromatin state dynamics in nine human cell types. *Nature* **473**, 43–49 (2011).
- Kataniemi, R. et al. CTCF/cohesin-binding sites are frequently mutated in cancer. *Nat. Genet.* **47**, 818–821 (2015).
- Lovén, J. et al. Selective inhibition of tumor oncogenes by disruption of super-enhancers. *Cell* **153**, 320–334 (2013).
- Khurana, E. et al. Role of non-coding sequence variants in cancer. *Nat. Rev. Genet.* **17**, 93–108 (2016).
- Flavahan, W. A. et al. Insulator dysfunction and oncogene activation in IDH mutant gliomas. *Nature* **529**, 110–114 (2016).
- Melnikov, A. et al. Systematic dissection and optimization of inducible enhancers in human cells using a massively parallel reporter assay. *Nat. Biotech.* **30**, 271–277 (2012).
- Kwasniewski, J. C., Fiore, C., Chaudhari, H. G. & Cohen, B. A. High-throughput functional testing of ENCODE segmentation predictions. *Genome Res.* **24**, 1595–602 (2014).
- Arnold, C. D. et al. Genome-wide quantitative enhancer activity maps identified by STARR-seq. *Science* **339**, 1074–1077 (2013).
- Zabidi, M. A. et al. Enhancer-core-promoter specificity separates developmental and housekeeping gene regulation. *Nature* **518**, 556–559 (2015).
- van Arensbergen, J. et al. Genome-wide mapping of autonomous promoter activity in human cells. *Nat. Biotech.* **35**, 145–153 (2017).
- Maston, G. A., Evans, S. K. & Green, M. R. Transcriptional regulatory elements in the human genome. *Annu. Rev. Genomics Hum. Genet.* **7**, 29–59 (2006).
- Siu, G., Wurster, A. L., Duncan, D. D., Soliman, T. M. & Hedrick, S. M. A transcriptional silencer controls the developmental expression of the CD4 gene. *EMBO J.* **13**, 3570–3579 (1994).
- Sawada, S., Scarborough, J. D., Killeen, N. & Littman, D. R. A lineage-specific transcriptional silencer regulates CD4 gene expression during T lymphocyte development. *Cell* **77**, 917–929 (1994).
- Zou, Y.-R. et al. Epigenetic silencing of CD4 in T cells committed to the cytotoxic lineage. *Nat. Genet.* **29**, 332–336 (2001).
- Taniuchi, I. et al. Differential requirements for runx proteins in CD4 repression and epigenetic silencing during T lymphocyte development. *Cell* **111**, 621–633 (2002).
- Taniuchi, I., Sunshine, M. J., Festenstein, R. & Littman, D. R. Evidence for distinct CD4 silencer functions at different stages of thymocyte differentiation. *Mol. Cell* **10**, 1083–1096 (2002).
- Pang, B. et al. Direct antigen presentation and gap junction mediated cross-presentation during apoptosis. *J. Immunol.* **183**, 1083–1090 (2009).
- Straathof, K. C. et al. An inducible caspase 9 safety switch for T-cell therapy. *Blood* **105**, 4247–4254 (2005).
- Thurman, R. E. et al. The accessible chromatin landscape of the human genome. *Nature* **489**, 75–82 (2012).
- Giresi, P. G., Kim, J., McDaniell, R. M., Iyer, V. R. & Lieb, J. D. FAIRE (Formaldehyde-Assisted Isolation of Regulatory Elements) isolates active regulatory elements from human chromatin. *Genome Res.* **17**, 877–885 (2007).
- Li, W. et al. MAGECK enables robust identification of essential genes from genome-scale CRISPR/Cas9 knockout screens. *Genome Biol.* **15**, 554 (2014).
- Robinson, M. D., McCarthy, D. J. & Smyth, G. K. edgeR: a Bioconductor package for differential expression analysis of digital gene expression data. *Bioinformatics* **26**, 139–140 (2010).
- Di, Y., Schafer, D. W., Cumbie, J. S. & Chang J. H. The NBP negative binomial model for assessing differential gene expression from RNA-seq. *Stat. Appl. Genet. Mol. Biol.* <https://doi.org/10.2202/1544-6115.1637> (2011).
- Visel, A. et al. ChIP-seq accurately predicts tissue-specific activity of enhancers. *Nature* **457**, 854–858 (2009).
- Bonn, S. et al. Tissue-specific analysis of chromatin state identifies temporal signatures of enhancer activity during embryonic development. *Nat. Genet.* **44**, 148–156 (2012).
- Dahlman, J. E. et al. Orthogonal gene knockout and activation with a catalytically active Cas9 nuclease. *Nat. Biotechnol.* **33**, 1159–1161 (2015).
- Konermann, S. et al. Genome-scale transcriptional activation by an engineered CRISPR-Cas9 complex. *Nature* **517**, 583–588 (2015).
- Calderwood, D. A., Shattil, S. J. & Ginsberg, M. H. Integrins and actin filaments: reciprocal regulation of cell adhesion and signaling. *J. Biol. Chem.* **275**, 22607–22610 (2000).
- Shlyueva, D., Stampfel, G. & Stark, A. Transcriptional enhancers: from properties to genome-wide predictions. *Nat. Rev. Genet.* **15**, 272–286 (2014).
- Ernst, J. & Kellis, M. ChromHMM: automating chromatin state discovery and characterization. *Nat. Methods* **9**, 215–216 (2012).
- Yu, G., Wang, L. G. & He, Q. Y. ChIPseeker: an R/Bioconductor package for ChIP peak annotation, comparison and visualization. *Bioinformatics* **31**, 2382–2383 (2015).
- Beck, D. B., Oda, H., Shen, S. S. & Reinberg, D. PR-Set7 and H4K20me1: at the crossroads of genome integrity, cell cycle, chromosome condensation, and transcription. *Genes Dev.* **26**, 325–337 (2012).
- Chantalat, S. et al. Histone H3 trimethylation at lysine 36 is associated with constitutive and facultative heterochromatin. *Genome Res.* **21**, 1426–1437 (2011).
- Ahn, S. H., Kim, M. & Buratowski, S. Phosphorylation of Serine 2 within the RNA polymerase II C-terminal domain couples transcription and 3' end processing. *Mol. Cell* **13**, 67–76 (2004).
- Liu, T. et al. Cistrome: an integrative platform for transcriptional regulation studies. *Genome Biol.* **12**, R83–R83 (2011).
- Jiang, J. G., DeFrances, M. C., Machen, J., Johnson, C. & Zarnegar, R. The repressive function of AP2 transcription factor on the hepatocyte growth factor gene promoter. *Biochem. Biophys. Res. Commun.* **272**, 882–886 (2000).
- Eckert, D., Buhl, S., Weber, S., Jäger, R. & Schorle, H. The AP-2 family of transcription factors. *Genome Biol.* **6**, 246 (2005).
- Roth, C., Schuierer, M., Günther, K. & Buettner, R. Genomic structure and DNA binding properties of the human zinc finger transcriptional repressor AP-2rep (KLF12). *Genomics* **63**, 384–390 (2000).
- Bonev, B. & Cavalli, G. Organization and function of the 3D genome. *Nat. Rev. Genet.* **17**, 661–678 (2016).
- Krijger, P. H. L. & de Laat, W. Regulation of disease-associated gene expression in the 3D genome. *Nat. Rev. Mol. Cell Biol.* **17**, 771–782 (2016).
- Rao, S. S. et al. A 3D map of the human genome at kilobase resolution reveals principles of chromatin looping. *Cell* **159**, 1665–1680 (2014).
- Wang, Y. et al. The 3D Genome Browser: a web-based browser for visualizing 3D genome organization and long-range chromatin interactions. *Genome Biol.* **19**, 151 (2018).
- Heidari, N. et al. Genome-wide map of regulatory interactions in the human genome. *Genome Res.* **24**, 1905–1917 (2014).
- Javierre, B. M. et al. Lineage-specific genome architecture links enhancers and non-coding disease variants to target gene promoters. *Cell* **167**, 1369–1384.e1319 (2016).
- Sanyal, A., Lajoie, B. R., Jain, G. & Dekker, J. The long-range interaction landscape of gene promoters. *Nature* **489**, 109–113 (2012).
- Hart, T., Komori, H. K., LaMere, S., Podshivalova, K. & Salomon, D. R. Finding the active genes in deep RNA-seq gene expression studies. *BMC Genomics* **14**, 778 (2013).
- Muerdter, F. et al. Resolving systematic errors in widely used enhancer activity assays in human cells. *Nat. Methods* **15**, 141–149 (2018).
- Wang, Y. M. et al. Correlation between DNase I hypersensitive site distribution and gene expression in HeLa S3 cells. *PLoS ONE* **7**, e42414 (2012).

58. Bell, O., Tiwari, V. K., Thomä, N. H. & Schübeler, D. Determinants and dynamics of genome accessibility. *Nat. Rev. Genet.* **12**, 554–564 (2011).
59. Evers, B. et al. CRISPR knockout screening outperforms shRNA and CRISPRi in identifying essential genes. *Nat. Biotechnol.* **34**, 631–633 (2016).
60. Morgens, D. W., Deans, R. M., Li, A. & Bassik, M. C. Systematic comparison of CRISPR/Cas9 and RNAi screens for essential genes. *Nat. Biotechnol.* **34**, 634–636 (2016).
61. Wijdeven, R. H. et al. Genome-wide identification and characterization of novel factors conferring resistance to topoisomerase II poisons in cancer. *Cancer Res.* **75**, 4176–4187 (2015).
62. Korkmaz, G. et al. Functional genetic screens for enhancer elements in the human genome using CRISPR-Cas9. *Nat. Biotechnol.* **34**, 192–198 (2016).
63. Boettcher, M. et al. Dual gene activation and knockout screen reveals directional dependencies in genetic networks. *Nat. Biotechnol.* **36**, 170–170 (2018).
64. Liao, H.-K. et al. In vivo target gene activation via CRISPR/Cas9-mediated trans-epigenetic modulation. *Cell* **171**, 1495–1507.e1415 (2017).
65. Matharu, N. et al. CRISPR-mediated activation of a promoter or enhancer rescues obesity caused by haploinsufficiency. *Science* **363**, eaau0629 (2019).
66. Komor, A. C., Badran, A. H. & Liu, D. R. CRISPR-based technologies for the manipulation of eukaryotic genomes. *Cell* **168**, 20–36 (2017).
67. Ma, H. et al. Correction of a pathogenic gene mutation in human embryos. *Nature* **548**, 413–419 (2017).
68. Gilbert, L. A. et al. Genome-scale CRISPR-mediated control of gene repression and activation. *Cell* **159**, 647–661 (2014).

Publisher's note Springer Nature remains neutral with regard to jurisdictional claims in published maps and institutional affiliations.

© The Author(s), under exclusive licence to Springer Nature America, Inc. 2020

Methods

Cell culture. K562 cells were cultured in RPMI 1640 with L-glutamine, 10% fetal bovine serum (FBS) and Pen-Strep. HepG2 cells were cultured in DMEM, 10% FBS and Antibiotic-Antimycotic. Cell density and culture conditions were maintained according to the ENCODE Cell Culture Guidelines.

Library construction. FAIRE was performed using K562 cells as previously described^{29,69,70}. Briefly, 5×10^7 K562 cells were fixed with a final concentration of 1% formaldehyde for 5 min, followed by the addition of 2.5 M glycine to a final concentration of 125 mM and cells were incubated for 5 min at room temperature while shaking. Cells were then lysed in 5 ml of lysis buffer 1 (50 mM HEPES-KOH, pH 7.5, 140 mM NaCl, 1 mM EDTA, 10% glycerol, 0.5% NP-40, 0.25% Triton X-100) and rocked at 4°C for 10 min. The tubes were subsequently centrifuged at 1,300g for 5 min at 4°C and the supernatant was removed. The pellet was suspended in 5 ml of lysis buffer 2 (10 mM Tris-HCl, pH 8.0, 200 mM NaCl, 1 mM EDTA, 0.5 mM EGTA), rocked at room temperature for 10 min, and centrifuged at 1,300g for 5 min at 4°C, and the supernatant was removed. The pellet was then suspended in 2 ml of lysis buffer 3 (10 mM Tris-HCl, pH 8.0, 100 mM NaCl, 1 mM EDTA, 0.5 mM EGTA, 0.1% Na-deoxycholate, 0.5% N-lauroylsarcosine). Cells were then sonicated in bioruptor tubes with sonication beads for 16 cycles for 30 s each followed by 30-s incubation periods at 4°C. The tubes were centrifuged at 3,000 r.p.m. for 5 min at 4°C, an equal volume of phenol/chloroform (phenol, chloroform and isoamyl alcohol 25/24/1 saturated with 10 mM Tris, pH 8.0, 1 mM EDTA) was added to the lysate and the aqueous phase was separated with phase lock gel. DNA from the aqueous phase was then precipitated with ethanol at -80°C. The pelleted DNA was reverse cross-linked and processed according to the Illumina sequencing library preparation protocol. After Illumina adapters were ligated, fragments were size-selected for 200 bp. PCR procedures using Phusion High-Fidelity PCR2x Master Mix and PCR primers 1.0 and 2.0 for Illumina TruSeq adapters were: 98°C for 30 s, 12 cycles of 98°C for 10 s, 65°C for 30 s and 72°C for 30 s, and 72°C for 5 min. Half of the fragments were further processed for next-generation sequencing using the Illumina MiSeq platform, to confirm that the FAIRE process had enriched the proper open chromatin regions. The other half was amplified using primers containing additional sequences by PCR for downstream Gibson assembly. Primer sequences for using Phusion High-Fidelity PCR2x Master were: *ACTCCTTTCAAGACCTAGCTCAAGCAGAAGACGGCATAACGAGAT*; *ATCCAGTTTGTTTAATTAAGAATGATACGGCGACCGAGATCTACACTCTTTCCCTAC*. PCR procedures were: 98°C for 30 s, 8 cycles of 98°C for 10 s, 65°C for 30 s and 72°C for 30 s, and 72°C for 5 min. These fragments were then gel-purified.

The ReSE screen lentivirus vector pLenti-FKBP-delCasp9-Puro was designed based on plasmids from Addgene (nos. 15567 and 52961)^{27,71}. EF-1 α , a human constitutive promoter, was used to drive the expression of FKBP-Casp9 and the UbC promoter was used to drive the expression of a puromycin-resistance gene. We reasoned that strong silencer activity would have limited effects on the virus packaging and subsequent puromycin selection, as shown in a retrospective experiment that virus titer and the subsequent puromycin selection were not affected by silencer insertions in the screen plasmid (Supplementary Fig. 11). However, we cannot rule out that there might exist 'super-silencer' fragments that would affect virus production or puromycin expression. pLenti-FKBP-delCasp9-Puro plasmids were digested with BsmBI enzyme and gel-purified. The FAIRE fragments were then inserted into the digested plasmids, 15 bp upstream of the EF-1 α using Gibson Assembly. The rationale was to identify a class of strong and more general silencers that are able to repress transcription upstream of the constitutive promoter EF-1 α . The assembly mix was made using 50 ng of insert DNA, 50 ng of digested plasmids and 10 μ l of 2x Gibson Assembly Master Mix to produce a final volume of 20 μ l. The assembly mix was incubated at 50°C for 60 min, then 2 μ l of the mix was electroporated into 25 μ l of Endura electrocompetent cells to test the transformation efficiency. The electroporation was scaled to reach approximately 160,000 colonies, which were plated on four 245-mm Petri dishes with 100 μ g ml⁻¹ carbenicillin. Colonies were then scraped and plasmid DNA extracted using the Qiagen Maxiprep Kit.

Lentivirus production and infection. The 293T cells were grown in five T175 flasks at 50% confluency before transfection. For each flask of 293T cells grown in 25 ml of fresh medium, 15 μ g of library plasmids, 10 μ g of psPAX2, 5 μ g of pCMV-VSV-G and 90 μ l of X-tremeGENE 9 DNA Transfection Reagent were mixed in 1 ml of serum-free medium and used for transfection. Fresh medium was added the day following transfection. Media supernatant containing virus particles was collected on the second and third days after transfection, pooled and further concentrated using Lenti-X according to the manufacturer's protocol. Virus titer was then determined by making serial (10^{-3} to 10^{-10}) dilutions of 4 μ l of frozen virus supernatant in media containing 8 μ g ml⁻¹ of polybrene to infect 293T cells. Two days after infection, cells were selected with 2 μ g ml⁻¹ puromycin for an additional 7 d. Virus titer was then calculated based on the survival colonies and the related dilution. K562 cells and HepG2 cells were then infected with the same virus library at multiplicity of infection = 0.5 by spin-infection. For spin-infection, 3×10^6 cells in each well of a 12-well plate were infected in 1 ml of medium containing 8 μ g ml⁻¹ of polybrene. In total, four plates were used for each infection to analyze a total

of 1.5×10^8 cells. Two days after infection, cells were selected by 2 mg ml⁻¹ of puromycin for a further 5 d. For each biological replicate experiment of both K562 and HepG2 cells, the infection was repeated and cells were infected with lentivirus from the same pool of virus containing the same library content.

Silencer screen. After puromycin selection, 3.5×10^8 K562 cells were frozen as non-treated control. A separate aliquot of 3.5×10^8 cells was treated with 1 nM of AP20187 for 18 h to induce apoptosis. Dead cells were then removed with a Dead Cell Removal Kit (Miltenyi Biotec). In the screen of K562 cells, we retrieved 45.6% of live cells compared to the original input cell number after 18 h of AP20187 treatment. When cell growth of the live cells during this 18-h period is also considered, the real survival rate should be around 30.4% (considering that the normal doubling time of live K562 cells is 24 h). In addition, there are also some other scenarios—for example, although cells with virus infection survived puromycin selection (as expression of the puromycin-resistance gene is under another independent promoter, UbC), the expression of FKBP-Casp9 was silenced by other machinery within the cells. Alternatively, cells were still in the early stage of apoptosis and were not removed by the live cell isolation method. These are potential reasons for the higher survival rates noted. Many such false-positive regions were removed during biological repeat experiments. Live cells were further grown for a further 5 d. Genomic DNA from 3.5×10^8 cells of non-treated control cells or post-apoptosis-induction cells was isolated using the QIAamp DNA Blood Maxi Kit, with two columns per treatment. For the K562 cell differentiation test, the same batches of cells that were analyzed as biological replicates were recovered from cells frozen in 10% DMSO. Cells were then differentiated with 10 nM PMA for 2 d. Cells were divided into differentiated non-treated control cells while the other half was treated with 1 nM AP20187 for 18 h to induce apoptosis. Dead cells were cleared as described previously. For HepG2 cells, the experimental procedures were similar except that dead cells were removed by removal of the media, since HepG2 cells are adherent cells and live cells remained attached to the tissue culture flasks.

Library sequencing and analyses. Genomic DNA containing the ReSE lentivirus inserts was amplified by PCR using Illumina PCR primers 1.0 and 2.0. For each 100- μ l PCR reaction, 10 μ g of genomic DNA, 20 μ l of 5x Phusion HF buffer, 2 μ l of 10 mM deoxynucleotide triphosphate, 2.5 μ l of Phusion polymerase, 5 μ l of 25 μ M 1.0 primer and 5 μ l of 25 μ M 2.0 primer were used. For each treatment sample, 16 reactions were prepared and pooled. PCR procedures were: 98°C for 30 s, 20 cycles of 98°C for 10 s, 65°C for 30 s and 72°C for 30 s, and 72°C for 5 min. PCR products were then size-selected and purified. Final products were sequenced on either an Illumina MiSeq or HiSeq4000 platform. Sequence reads were aligned using Bowtie2. Approximately 100,000 regions of the 177,000 within the library were estimated to be well covered in the screen. A GFF file was made from aligned reads pooled from all experiments. Read counts (quality ≥ 30) were then calculated using HTSeq⁷². Final enrichment was calculated by MAGeCK³⁰, with two biological replicates for each condition. Briefly, read counts derived from HTSeq of different samples were first median-normalized to adjust for the effect of library sizes and read count distributions. The variance of read counts was then estimated by sharing information across features, and a negative binomial model was used to test whether fragment abundance differed significantly between post-apoptosis-induction and control replicates. *P* values were calculated from the negative binomial model using a modified robust ranking aggregation algorithm³⁰. FDR was then computed from the empirical permutation *P* values using the Benjamini-Hochberg procedure³⁰. Because fold enrichments are only semi-quantitative, fragments with FDR < 0.01 were considered as significant hits for downstream analyses and the list of silencers was sorted based on FDR values from low to high.

Luciferase assay. Candidate silencer sequences were amplified with primers containing a homologous arm using PCR from the genomic DNA of K562 cells. These fragments were then inserted in front of the PGK promoter of the luciferase plasmid pGL4.53 (Promega) using Gibson assembly. Cells were then co-transfected with the pRL-CMV *Renilla* reporter vector and the pGL4.53 vector with the silencer sequence inserted. The luciferase assay was performed using the Dual-Glo Luciferase Assay Kit from Promega according to the manufacturer's protocol. Original luciferase plasmid without any insertion was used as the control. All luciferase assays were from three independent transfections performed on different days. All tested regions and associated primers are listed in Supplementary Table 9.

Pathway analyses. Proximal genes around silencers were defined as either (1) the presence of silencers in the promoter regions only (10 kb surrounding TSS) or (2) the presence of silencers in both promoter regions (1 kb surrounding TSS) and gene bodies. Pathway analyses were performed using proximal genes with ingenuity pathway analysis.

CRISPR-Cas9-guided silencer knockout. Guide RNAs targeting the 5' and 3' ends of the silencer were designed using Zhang Lab (<http://crispr.mit.edu/>). The gRNA sequence was cloned into the PX459V2 plasmid containing the gRNA scaffold and Cas9 sequence. Two CRISPR-Cas9 plasmids targeting both the 5' and 3' end of the

silencer were co-transfected into the cells. Cells were then selected for successful transfection using puromycin. Single clones of cells were picked and verified using PCR and Sanger sequencing. Gene expression of target genes was quantified using qPCR, and normalized to the expression of the housekeeping gene *GAPDH*. All tested regions and associated primers are listed in Supplementary Table 9.

Downstream informatic analyses. Genomic annotation of silencer regions was analyzed using the R packages ChIPseeker and CEAS^{40,73}. Motif analyses were performed using Cistrome⁶⁹. For Motif analyses, only those silencers outside the promoter regions were used for analyses to reduce bias from motif-rich promoter regions, though we did not observe major differences using all silencers or only silencers outside of the promoter regions for motif analyses. Region intersections, comparisons, binomial testing and other downstream analyses were calculated using R, ChIPpeakAnno, Galaxy or Cistrome^{44,74,75}. Enrichment of chromatin states was calculated using a one-sided binomial test against the whole ReSE library as the background. ChIP-seq data from ENCODE and dbSNP147 data were downloaded from the UCSC Genome Browser Database with the hg19 genome assembly⁶. Association of histone modifications and transcription factor binding regions with silencers was calculated using ChIPseeker⁴⁰. Enrichment analysis was based on permutation tests using 20,000 random permutations. The *P* value was then calculated and multiple comparison corrections were computed using the Benjamini–Hochberg procedure for the adjusted *P* value⁴⁰. For comparison of silencers with capture Hi-C data from human primary blood cells⁵³ or 5C data from K562 cells⁵⁴, silencer regions identified from the ReSE screen in K562 cells were intersected with the distal regions that interacted with the promoter regions from the respective studies. Hi-C, ChIA-PET and 5C data of K562 cells were used and visualized using genome browsers^{50–52,54,77}.

Reporting Summary. Further information on research design is available in the Nature Research Reporting Summary linked to this article.

Data availability

The sequencing data are available at GEO under accession number [GSE108536](https://www.ncbi.nlm.nih.gov/geo/query/acc.cgi?acc=GSE108536). Source data for Figs. 1–5 and Extended Data Figs. 2, 3, 6, 7, 9 and 10 are available with the paper.

References

69. Pang, B. et al. Drug-induced histone eviction from open chromatin contributes to the chemotherapeutic effects of doxorubicin. *Nat. Commun.* **4**, 1908 (2013).
70. Giresi, P. G. & Lieb, J. D. Isolation of active regulatory elements from eukaryotic chromatin using FAIRE (Formaldehyde Assisted Isolation of Regulatory Elements). *Methods* **48**, 233–239 (2009).
71. Sanjana, N. E., Shalem, O. & Zhang, F. Improved vectors and genome-wide libraries for CRISPR screening. *Nat. Methods* **11**, 783–784 (2014).
72. Anders, S., Pyl, P. T. & Huber, W. HTSeq—a Python framework to work with high-throughput sequencing data. *Bioinformatics* **31**, 166–169 (2015).
73. Ji, X., Li, W., Song, J., Wei, L. & Liu, X. S. CEAS: cis-regulatory element annotation system. *Nucleic Acids Res.* **34**, W551–W554 (2006).
74. Zhu, L. J. et al. ChIPpeakAnno: a Bioconductor package to annotate ChIP-seq and ChIP-chip data. *BMC Bioinf.* **11**, 237 (2010).
75. Giardine, B. et al. Galaxy: a platform for interactive large-scale genome analysis. *Genome Res.* **15**, 1451–1455 (2005).
76. Karolchik, D., Hinrichs, A. S. & Kent, W. J. The UCSC genome browser. *Curr. Protoc. Bioinformatics* **28**, 1.4 (2009).
77. Zhou, X. & Wang, T. Using the Wash U epigenome browser to examine genome-wide sequencing data. *Curr. Protoc. Bioinformatics* **40**, 10.10 (2012).

Acknowledgements

We thank J. Gruber, X. Li, E. Monte, K. Van Bortle, C. Jiang and M. Shi at Stanford University, and L. Janssen, Y. Li, L. Hamoen and A. Henic at Leiden University Medical Center, for many helpful discussions and inputs regarding the manuscript. This work was supported by the National Institutes of Health (NIH; nos. U54HG006996 and UM1HG009442) to M.P.S. This work used the Genome Sequencing Service Center of Stanford Center for Genomics and Personalized Medicine Sequencing Center, supported by NIH grant award nos. S10OD020141 and S10OD025212. B.P. was partially supported by the LUMC Gisela Thier Fellowship and KWF/Alpe Young Investigator Grant no. 11707.

Author contributions

B.P. and M.P.S. conceived the project. B.P. designed and performed experiments and analyses. B.P. and M.P.S. wrote the manuscript.

Competing interests

M.P.S. is a founder and member of the science advisory board of Personalis, SensOmics, Qbio, January, Mirvie and Filtricine, and a science advisory board member of Genapsys and Epinomics.

Additional information

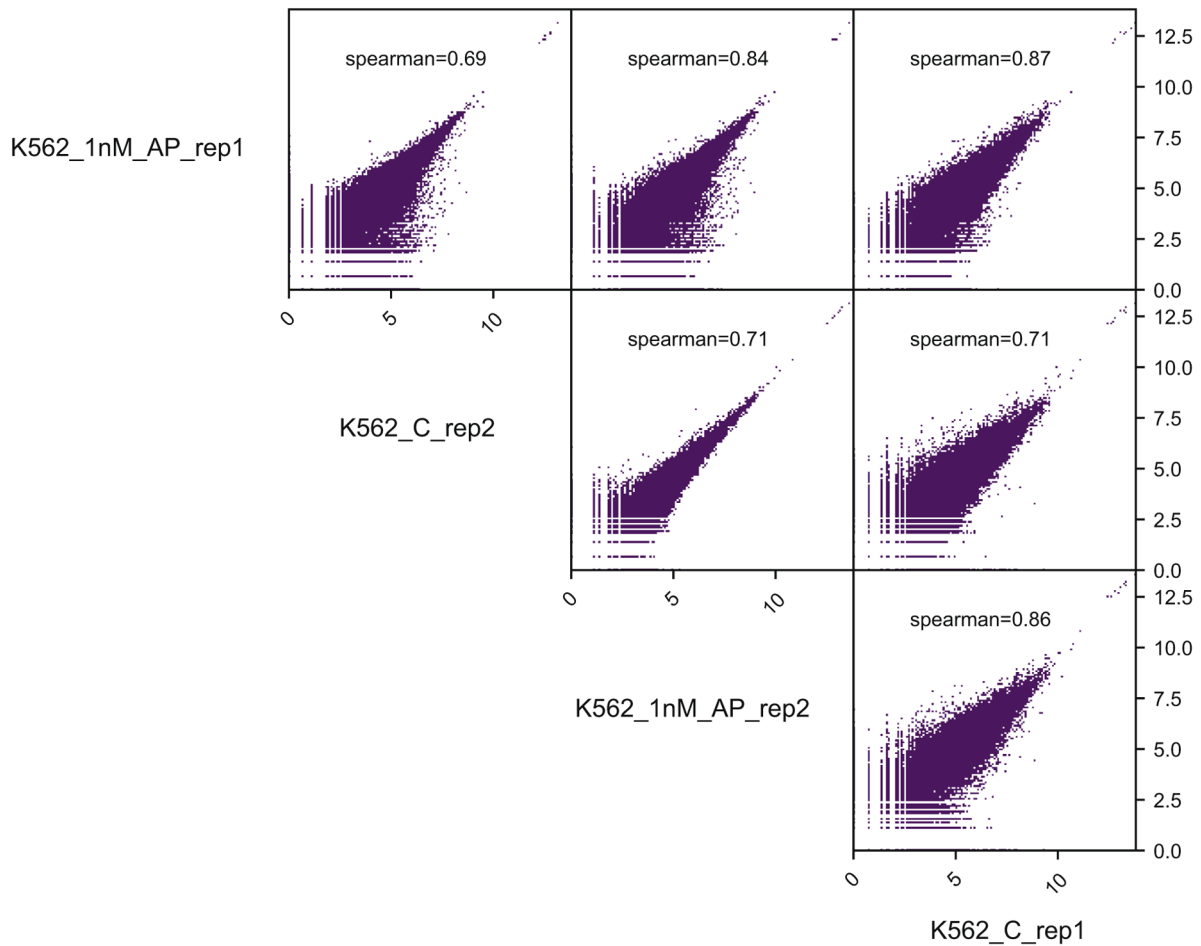
Extended data is available for this paper at <https://doi.org/10.1038/s41588-020-0578-5>.

Supplementary information is available for this paper at <https://doi.org/10.1038/s41588-020-0578-5>.

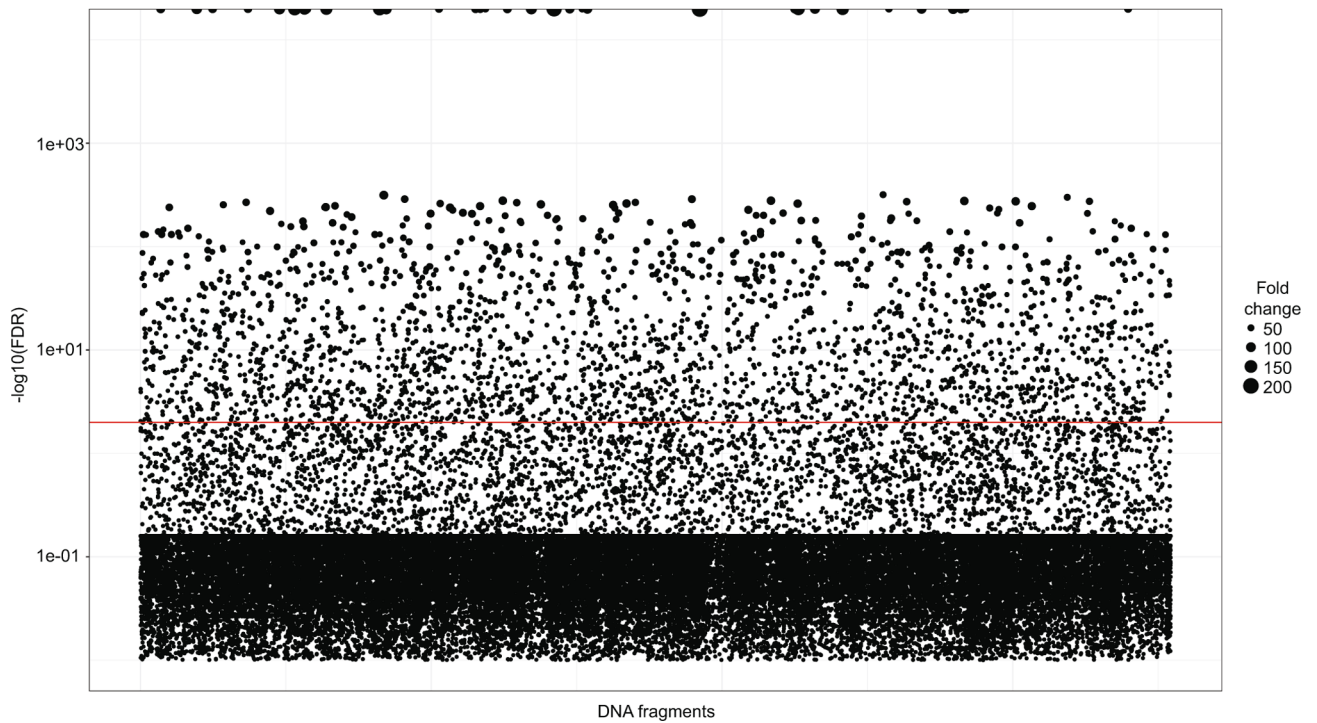
Correspondence and requests for materials should be addressed to M.P.S.

Reprints and permissions information is available at www.nature.com/reprints.

a

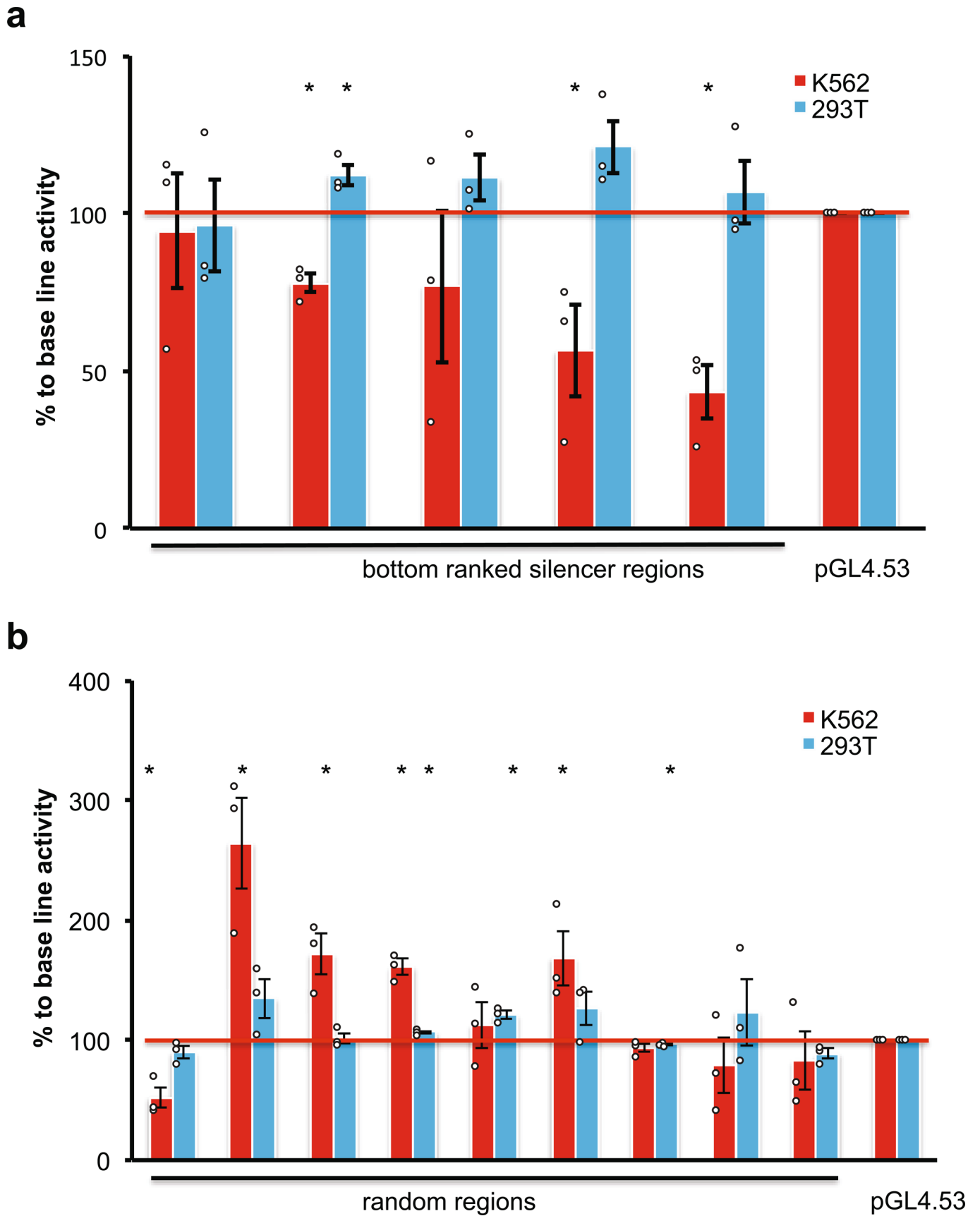


b



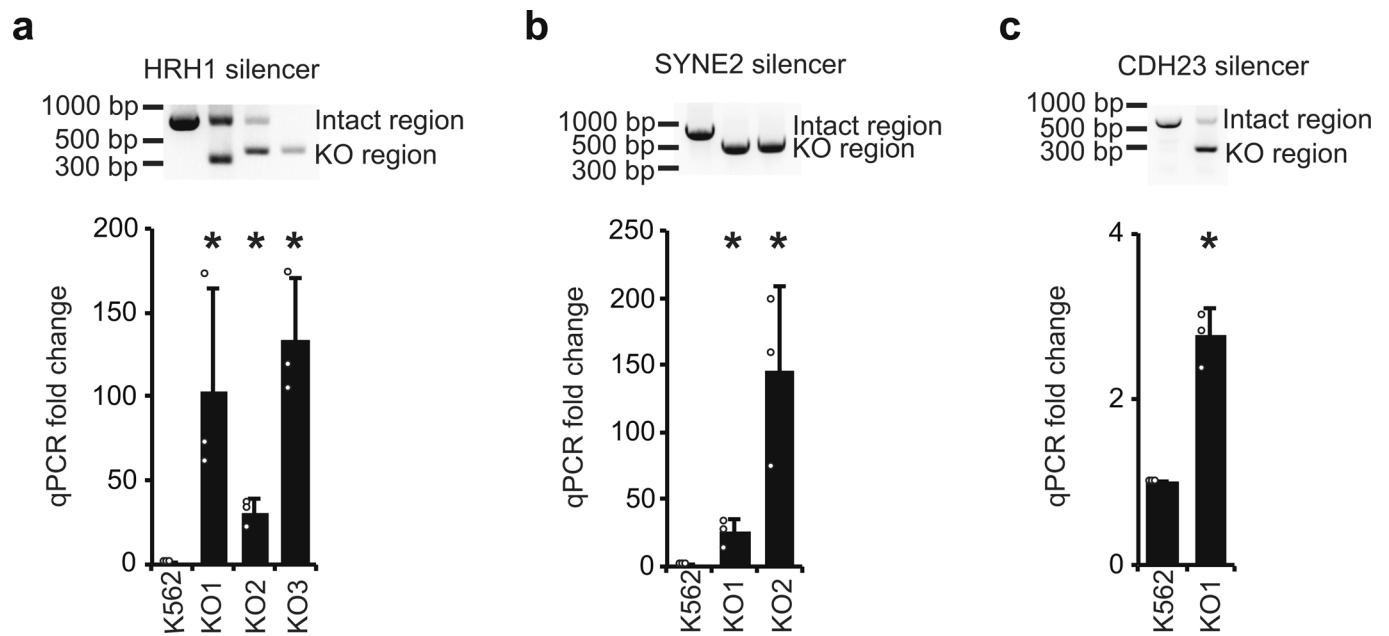
Extended Data Fig. 1 | See next page for caption.

Extended Data Fig. 1 | ReSE screen results from K562 cells. (a) The genome is split into bins of 1000 bp. For each bin, the number of reads found in each sample is counted. All regions were included. Spearman correlation was used to calculate the correlation efficiency among all 4 samples. **(b)** ReSE screen results from two biological replicate experiments in K562 cells. Each circle represents one tested fragment. The y-axis indicates the FDR of enrichment of the ReSE fragments after induction of apoptosis compared with untreated control cells. The size of the circle indicates the fold enrichment of ReSE fragment counts of apoptosis-induction samples over untreated control after normalization. The red line indicates the cutoff value of FDR at 0.01.

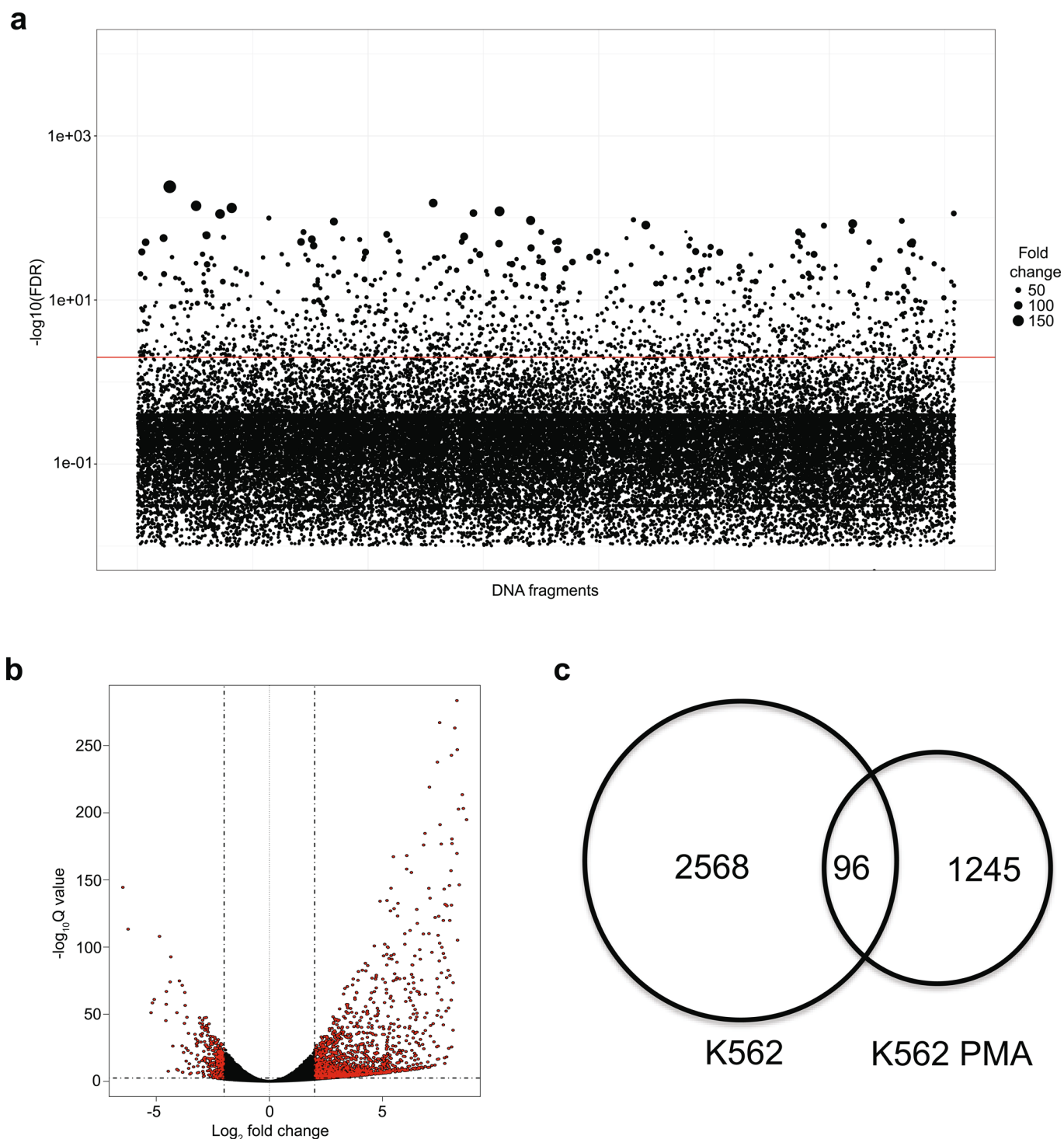


Extended Data Fig. 2 | See next page for caption.

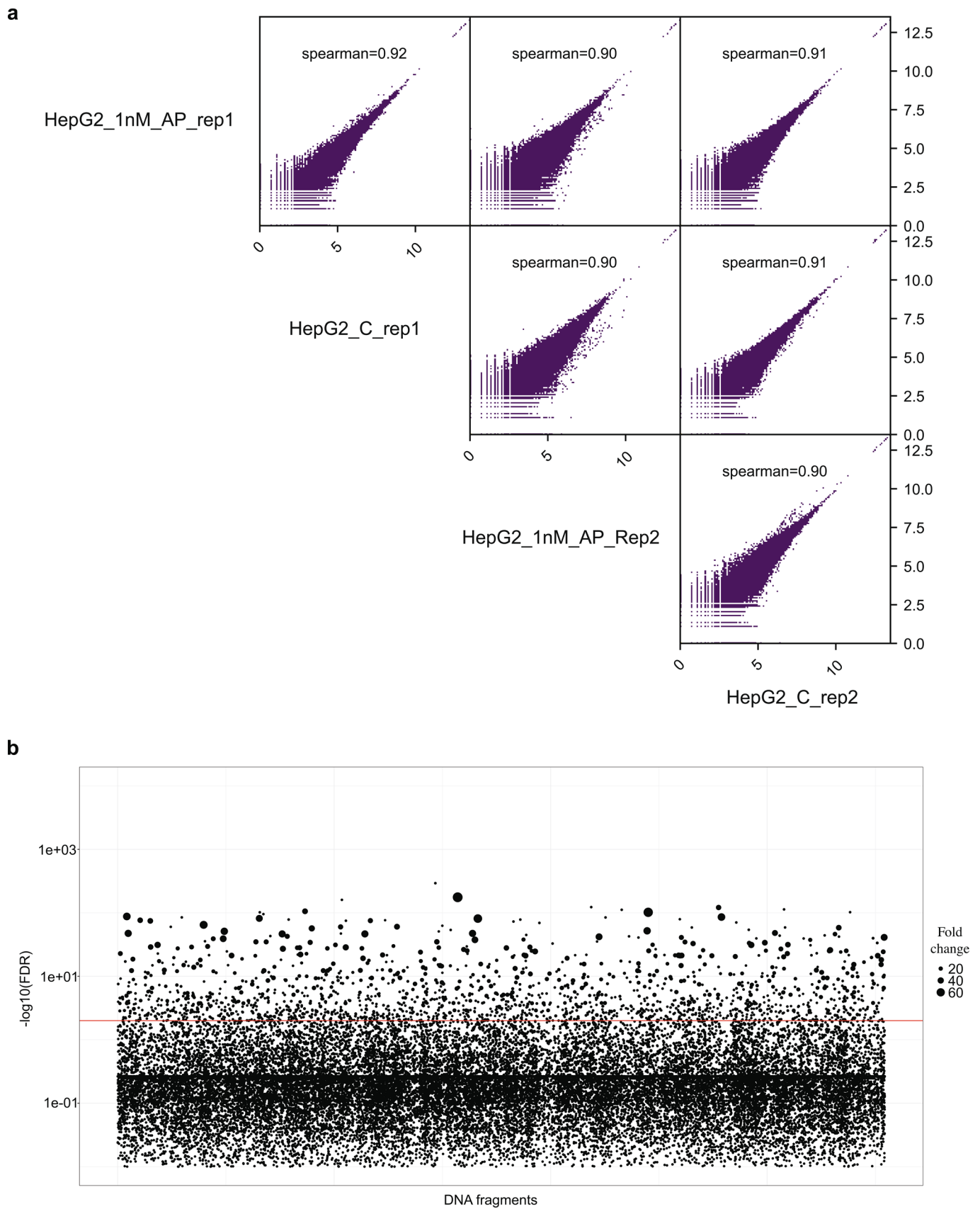
Extended Data Fig. 2 | Luciferase assays to determine the repressive activity of regions from K562 cells. Silencer regions ranked on the bottom of the list based on the FDR value **(a)** or random regions from the screen **(b)** were cloned by PCR from the genomic DNA of K562 cells, and then inserted upstream of the promoter of a luciferase reporter plasmid pGL4.53. The 293T cells were used as the control cell line to control for cell-type dependent repressive activity, and the empty pGL4.53 plasmid was used as the control for the baseline luciferase activity. The Y-axis represents the percentage of luciferase activity compared to the pGL4.53 empty plasmids in the respective cells ($n = 3$ biological independent samples; the bars show the mean value \pm S.E.M; * P value < 0.05 , calculated using two-sided Student's t test). All exact P values are provided in the Source Data.



Extended Data Fig. 3 | Gene up-regulation by removing silencers from endogenous regions in K562 cells. Three silencers from (Fig. 1e) are in the intron regions of genes *HRH1* (a), *SYNE2* (b) and *CDH23* (c). Paired CRISPR guide RNAs were designed to target both sides of the selected silencer to remove it from the endogenous locus. Single clones were selected and verified by PCR (upper panel), which is the representative result of 2 experiments. The expression of the respective genes was quantified by qPCR (lower panel). (n = 3 biological replicates of the same clones; the bars show the mean value \pm S.D.; *P value < 0.05, calculated using two-sided Student's *t* test). All exact *P* values are provided in the Source Data. The blots were cropped. Full scans of the blots are shown in Source Data Full Gel Extended Data Fig. 3.

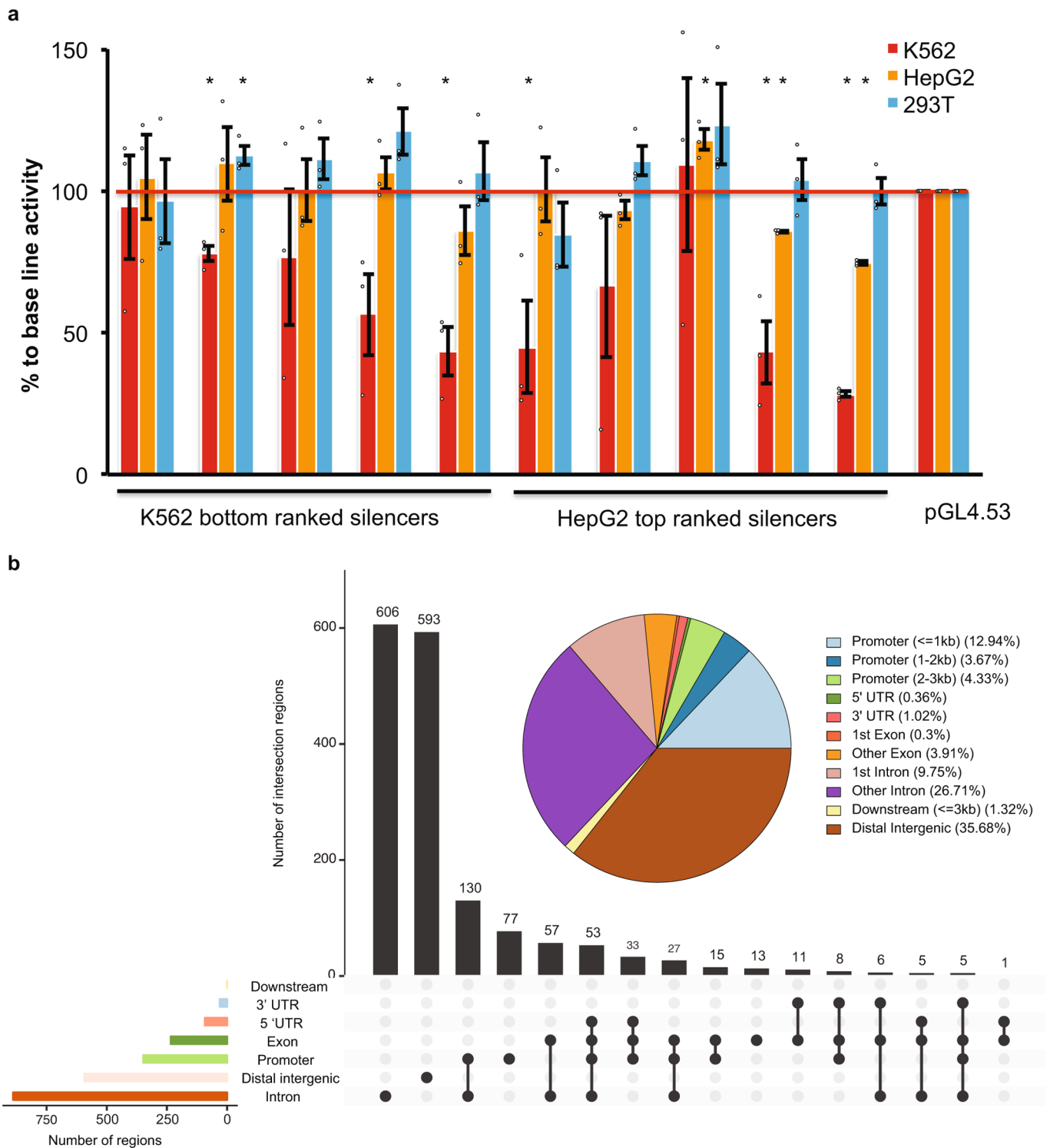


Extended Data Fig. 4 | ReSE screen results from K562 cells differentiated with PMA. (a) ReSE screen results from two biological replicate experiments in K562 cells treated with PMA. Each circle represents one tested fragment. The y-axis indicates the FDR of the enrichment of the ReSE fragments after induction of apoptosis compared with untreated control cells. The size of the circle indicates the fold enrichment of the ReSE fragment counts of the apoptosis-induction samples over the untreated control after normalization. The red line indicates the cutoff value of FDR at 0.01. **(b)** RNA-seq experiments were performed on the cell subsamples from (a). DESeq2 was used to calculate the genes deregulated in the cells with PMA treatment compared to the non-treated K562 cells. Around 4666 genes were changed at least 2 fold with the adjusted P value less than 0.01 during the PMA treatment (red dots). Two biological replicates were included for each condition. **(c)** Comparison of silencer regions identified from K562 cells and K562 cells differentiated by PMA. The overlapping was not random as determined by permutation tests ($n = 20,000$, adjust P value = 0.00005).

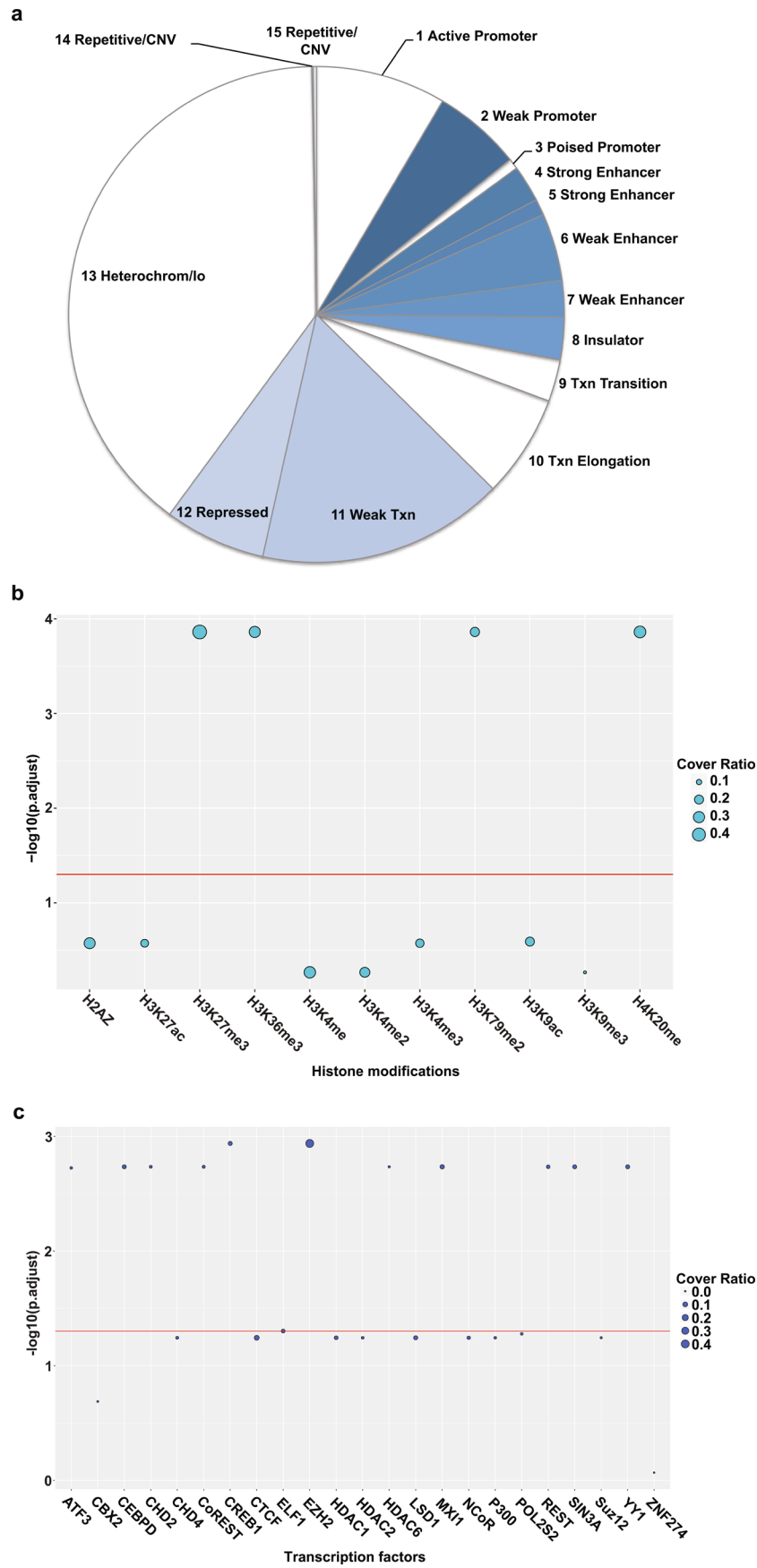


Extended Data Fig. 5 | See next page for caption.

Extended Data Fig. 5 | ReSE screen results from HepG2 cells. (a) The genome is split into bins of 1000 bp. For each bin, the number of reads found in each sample is counted. All regions were included. Spearman correlation was used to calculate the correlation efficiency among all 4 samples. **(b)** ReSE screen results from two biological replicate experiments in HepG2 cells. Each circle represents one tested fragment. The y-axis indicates the FDR of the enrichment of the ReSE fragments after induction of apoptosis compared with the untreated control cells. The size of the circle indicates the fold enrichment of ReSE fragment counts of the apoptosis-induction samples over the untreated control after normalization. The red line indicates the cutoff value of FDR at 0.01.

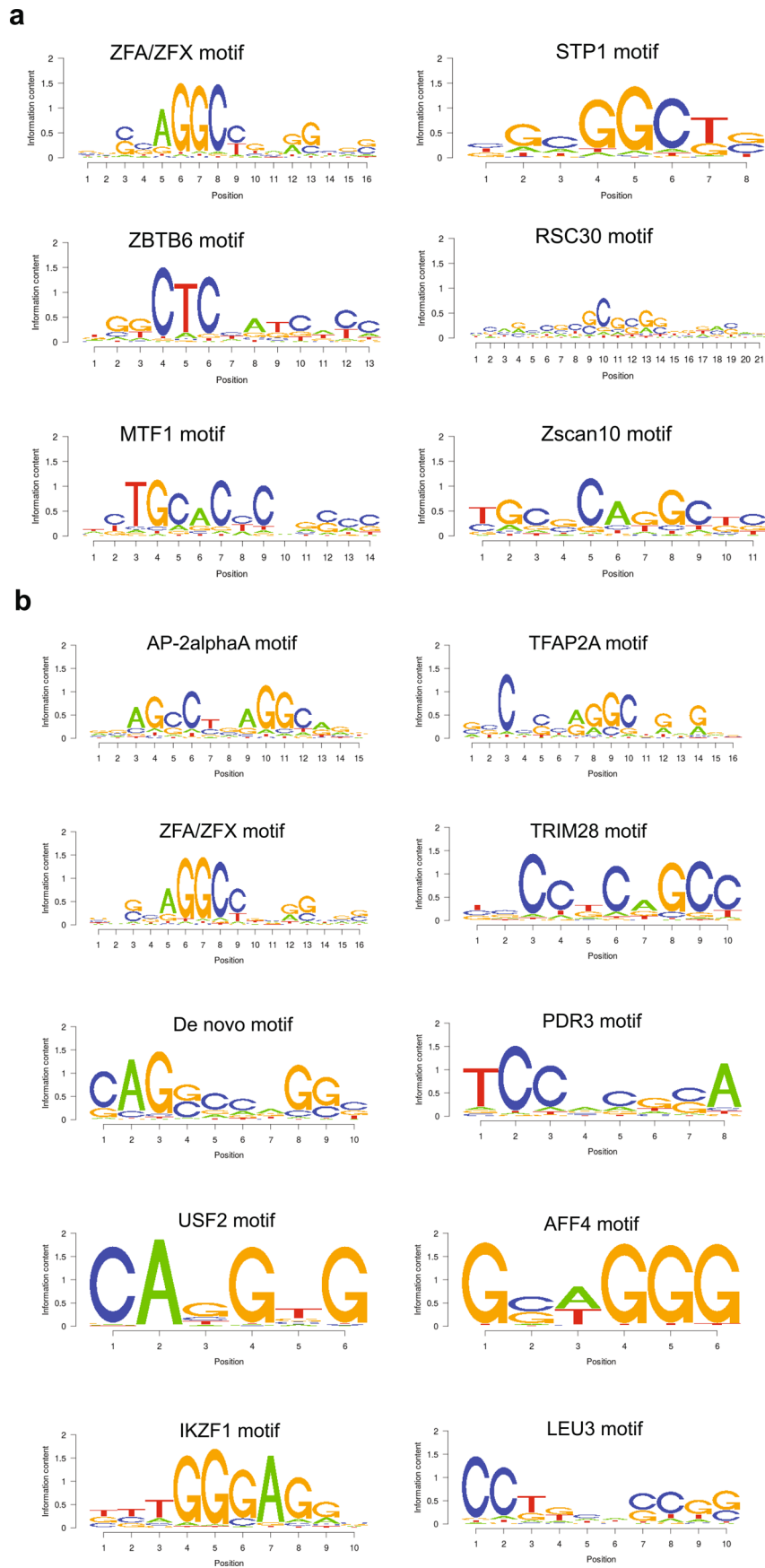


Extended Data Fig. 6 | Silencer regions identified from HepG2 cells. (a) Luciferase assays to determine the repressive activity of silencers from K562 and HepG2 cells. Silencer regions were cloned by PCR from the genomic DNA of K562 cells into a luciferase reporter plasmid pGL4.53. The 293T cells were used as the control cell line and the empty pGL4.53 plasmid was used as the control for the baseline luciferase activity. The Y-axis represents the percentage of luciferase activity compared to the pGL4.53 empty plasmids in the respective cells. Part of the data from K562 bottom ranked silencers were also used in Extended Data Fig. 2 ($n = 3$ biological independent samples; the bars show the mean value \pm S.E.M; * P value < 0.05 , calculated using two-sided Student's t test). **(b)** Distribution of the significantly enriched silencer regions from HepG2 cells in the genome. The pie chart indicates the distribution of silencers in genomic features. The bar plot indicates the distribution of silencers in the overlapping annotation features in the genome. All exact P values are provided in the Source Data.

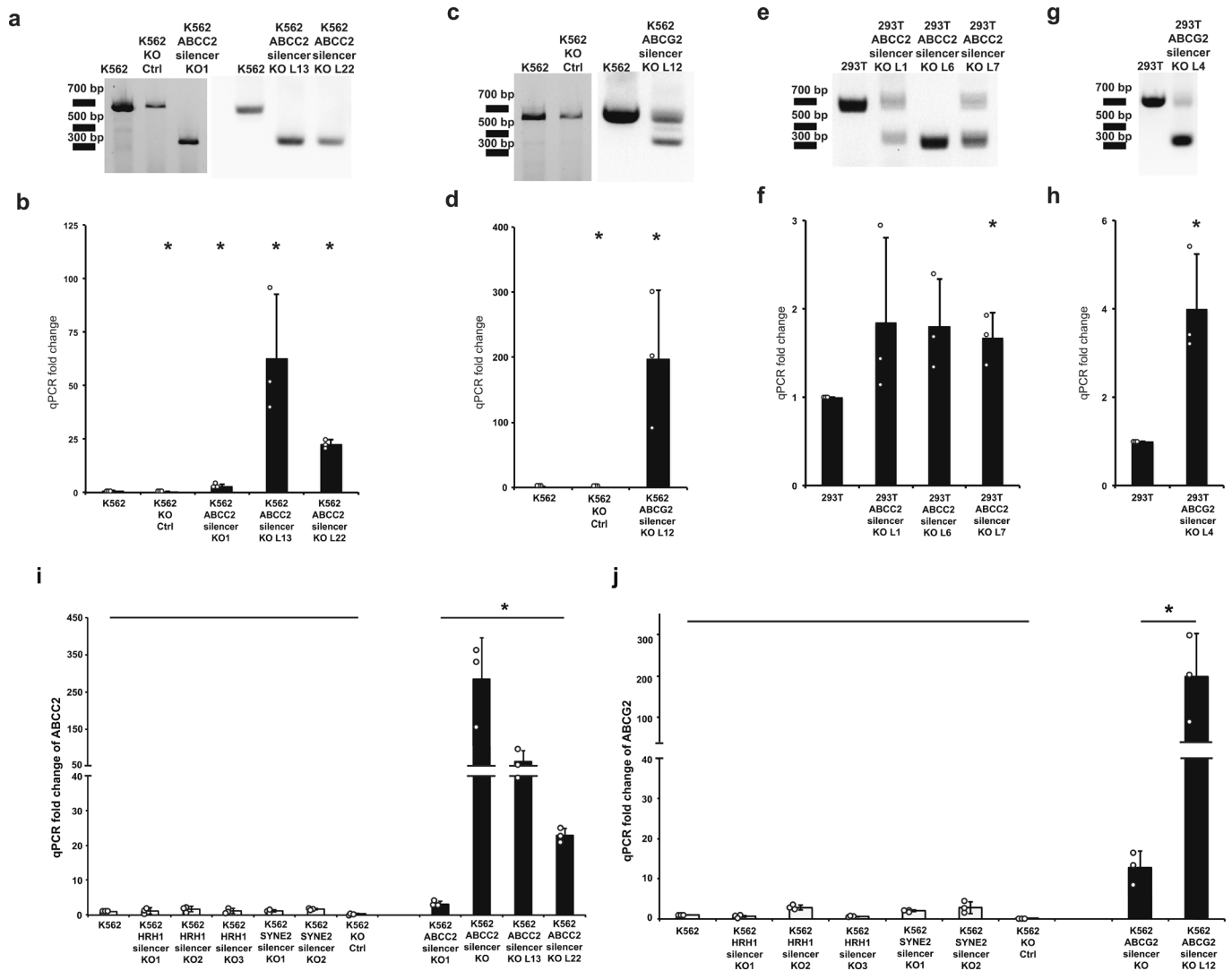


Extended Data Fig. 7 | See next page for caption.

Extended Data Fig. 7 | Unique signatures in silencer regions from HepG2 cells. (a) Distribution of silencer regions in the respective chromatin states in HepG2 cells. (Txn, transcription; Repressed, Polycomb repressed; lo, low signal; CNV, copy number variation). Colored wedges indicate the chromatin states that are significantly enriched compared to the library background distribution (P value < 0.001 , one-sided binomial test). **(b)** Association of histone modifications with silencers in HepG2 cells. The y-axis indicates the significance of the enrichment of histone modifications with silencer fragments. The size of the circle indicates the ratio of silencers covered by the respective histone modification (scale, 0-1). The enrichment analysis is based on permutation tests using 20,000 random permutations. The P values were calculated and multiple comparison corrections were computed using the Benjamini-Hochberg procedure. The red line shows the cutoff of the adjusted P value < 0.05 . **(c)** Association of transcription factors with silencers in HepG2 cells. The y-axis indicates the significance of the enrichment of transcription factors with silencer fragments. The size of the circle indicates the ratio of silencers covered by the respective transcription factor (scale, 0-1). The enrichment analysis is based on permutation tests using 20,000 random permutations. The P values were calculated and multiple comparison corrections were computed using the Benjamini-Hochberg procedure. The red line shows the cutoff of the adjusted P value < 0.05 . All exact P values are provided in the Source Data.



Extended Data Fig. 8 | Additional top motifs present in the silencer regions from K562 or HepG2 cells. Related to Fig. 3d,e,f. Top motifs identified in the silencers regions from K562 (a) or HepG2 (b) cells are shown.



Extended Data Fig. 9 | Additional silencer knockout clones from K562 and 293T cells. Related to Fig. 4c,d,e,f. Additional clones where silencer was knocked out from the *ABCC2* gene (a) or *ABCG2* gene (c) in K562 cells were generated, and confirmed by PCR. The expressions of *ABCC2* gene (b) and *ABCG2* gene (d) of the respective cells were quantified by qPCR. Clones where silencer was knocked out from the *ABCC2* gene (e) or *ABCG2* gene (g) in 293T cells were also generated, and confirmed by PCR. The expressions of *ABCC2* gene (f) and *ABCG2* gene (h) of the respective cells were quantified by qPCR (For all qPCR experiments, $n=3$ biological replicates of the same clones; the bars show the mean value \pm S.D.; * P value < 0.05 , calculated using two-sided Student's t test. All PCR experiments are the representative results of 2 experiments). (i and j) Silencer knockout clones (from Extended Data Fig. 3) were used as additional control knockout clones, since the targeted deletion regions were completely different from the *ABCC2* or *ABCG2* silencer regions. The expression of *ABCC2* (i) and *ABCG2* (j) genes of these clones was quantified by qPCR. The expression data of all individual clones were grouped as the control set, and compared to that of all the *ABCC2* or *ABCG2* silencer knockout clones (for each individual clone, $n=3$ biological replicates of the same clones; the bars show the mean value \pm S.D.). The *ABCC2* and *ABCG2* genes were significantly up-regulated in *ABCC2* silencer or *ABCG2* silencer knockout clones respectively (* P value < 0.05 , calculated using one-sided Student's t test). All exact P values are provided in the Source Data. The blots were cropped. Full scans of the blots are shown in Source Data Full Gel Extended Data Fig. 9.

